8) Whatley SD et al：Am I Hum Gnenet, **65**：984-994, 1999
9) Rossetti MV et al：BMC Med Genet, **9**：54, 2008
10) 野中薫雄ほか：日臨, **53**：1449-1455, 1995
11) Herbert A et al：Gastroenterology, **100**：1753-1757, 1991
12) Shehade SA et al：Clin Exp Dermatol, **16**：185-187, 1991
13) Meerman L et al：Transplantation, **57**：155-158, 1994

J. Biochem. 2011;149(2):153–160 doi:10.1093/jb/mvq126

JB THE JOURNAL OF BIOCHEMISTRY

Quinolone compounds enhance δ-aminolevulinic acid-induced accumulation of protoporphyrin IX and photosensitivity of tumour cells

Received September 10, 2010; accepted October 13, 2010; published online October 19, 2010

Yoshiko Ohgari[1], Yoshinobu Miyata[1], Tuan Thanh Chau[1], Sakihito Kitajima[1], Yasushi Adachi[2] and Shigeru Taketani[1,3,*]

[1]Department of Biotechnology Kyoto Institute of Technology, Kyoto 606-8585; [2]1st Department of Pathology, Kansai Medical University, Moriguchi, Osaka 570-8506; and [3]Department of Biotechnology, Kyoto Institute of Technology, Kyoto 606-8585, Japan

*Shigeru Taketani, Insect Biomedical Center, Kyoto Institute of Technology, Kyoto 606-8585, Japan. Tel: +81 75 724 7789, Fax: +81 75 724 7789, email: taketani@kit.ac.jp

Exogenous δ-aminolevulinic acid (ALA)-induced photodynamic therapy (PDT) has been used in the treatment of cancer. To obtain a high efficacy of ALA-PDT, we have screened various chemicals affecting ALA-induced accumulation of protoporphyrin in cancerous cells. When HeLa cells were treated with quinolone chemicals including enoxacin, ciprofloxacin or norfloxacin, the ALA-induced photodamage accompanied by the accumulation of protoporphyrin was stronger than that with ALA alone. Thus, quinolone compounds such as enoxacin, ciprofloxacin and norfloxacin enhanced ALA-induced photodamage. The increased ALA-induced photodamage in enoxacin-treated HeLa cells was decreased by haemin or ferric-nitrilotriacetate (Fe-NTA), suggesting that an increase in iron supply cancels the accumulation of protoporphyrin. On the other hand, the treatment of the cells with ALA plus an inhibitor of haem oxygenase, Sn-protoporphyrin, led to an increase in the photodamage and the accumulation of protoporphyrin compared with those upon treatment with ALA alone, indicating that the cessation of recycling of iron from haem augments the accumulation. The use of quinolones plus Sn-protoporphyrin strongly enhances ALA-induced photodamage. To examine the mechanisms involved in the increased accumulation of protoporphyrin, we incubated ferric chloride with an equivalent amount of quinolones. Iron–quinolone complexes with visible colours with a maximum at 450 nm were formed. The levels of iron-metabolizing proteins in enoxacin- or ciprofloxacin-treated cells changed, indicating that quinolones decrease iron utilization for haem biosynthesis. Hence, we now propose that the use of quinolones in combination with ALA may be an extremely effective approach for the treatment modalities for PDT of various tumour tissues in clinical practice.

Keywords: δ-aminolevulinic acid (ALA)/ciprofloxacin/enoxacin/PDT/photodamage/protoporphyrin/quinolones.

Abbreviations: ALA, δ-aminolevulinic acid; DMEM, Dulbecco's modified Eagle's medium; FCS, fetal calf serum; Fe-NTA, ferric-nitrilotriacetate; HO, haem oxygenase; MTT, 3-(4,5-dimethyl-thiazol-2-yl)-2,5-diphenyl-2*H*-tetrazolium bromide; PDT, photodynamic therapy; PVDF, poly(vinylidene difluoride); SDS–PAGE, sodium dodecylsulphate-polyacrylamide gel electrophoresis.

Photodynamic therapy (PDT) for cancer patients is widely used to treat non-melanoma skin tumours and preneoplastic skin lesions. PDT involves the activation of photosensitizer, which causes the release of singlet oxygen and other reactive oxygen species upon exposure to light, resulting in photodamage and subsequent tissue destruction (*1*). PDT is performed with ALA, which is converted to the active photosensitizer protoporphyrin IX within cells (*2*). In tumour cells, via the haem biosynthesis pathway, protoporphyrin is synthesized from a large amount of exogenous ALA and accumulates in a specific manner. The application of ALA following PDT treatment has been used in the treatment of skin diseases and has advantages over systemic administration in that the entire body does not face sensitization. ALA-induced PDT has been successfully applied in various medical fields including urology, gastroenterology and dermatology (*3*, *4*). Although there are reports that ALA-induced PDT can also be used as a fluorescence detection marker for the photodiagnosis of tumours (*5*, *6*), the mechanisms involved in the specific accumulation of protoporphyrin in cancerous tissues have not been clearly demonstrated. We previously reported that protoporphyrin accumulates owing to the limited capacity for ferrochelatase reaction (*7*, *8*) where the enzyme catalyses the insertion of ferrous ions into protoporphyrin IX to form protohaem. Additionally, we also reported the increase in the uptake of ALA by cancerous cells (*7*).

The death rate from non-melanoma skin cancer is reduced compared with that from other kinds of malignancies, but both mortality and incidence are rising in tropical regions and owing to the thinner ozone layer (*9*). Nonmelanoma skin cancer is classified into two general groups. One is basal cell carcinoma and the

other is squamous cell carcinoma (*10*). Although many studies on PDT carried out over the past decade show efficiency in treating non-melanoma skin cancer and preneoplastic skin lesion, the results of ALA-PDT in the treatment of them appear to be inadequate (*11*). Since ALA-PDT alone seems to be relatively insufficient for the treatment of non-melanoma skin cancer and preneoplastic skin lesion, advanced treatment options are required to significantly improve the therapeutic effectiveness of ALA-PDT.

Quinolone chemicals are widely used as synthetic anti-bacterial agents to treat respiratory tract infection (*12*). They have a broad anti-bacterial spectrum of activity against Gram-positive and -negative bacteria. Anti-bacterial activities of quinolones are involved in their inhibitory activities against DNA gyrase and topoisomerase IV (*13*, *14*). Both enzymes are members of the type II topoisomerase family that regulates bacterial DNA topology by passing a DNA double helix through another. In addition, the quinolones are used not only as anti-bacterial agents but also as an option for chemotherapy (*15*). During a study on enhancement of the phototoxic effect of ALA-induced photodamage, we tried to improve the sensitivity of ALA-PDT in cancerous cells by screening the increase in the accumulation of protoporphyrin, using many kinds of additional agents. We here report that quinolone agents including enoxacin and ciprofloxacin can enhance the accumulation of protoporphyrin as well as the photodamage in ALA-treated cancerous cells, and the importance of the recycling of iron from haem in cancerous cells upon ALA-induced photodamage is also shown.

Materials and Methods

Materials

Protoporphyrin IX and Sn-protoporphyrin were purchased from Frontier Scientific Co. (Logan, UT, USA). Enoxacin and lomefloxacin were products of Tokyo Kasei Chemicals (Tokyo, Japan) and Merck Biosciences (Darmstadt, Germany), respectively. Norfloxacin, and ciprofloxacin were from WAKO Chemicals (Tokyo). The antibodies for ferrochelatase and actin used were as previously described (*7*, *16*). Anti-transferrin receptor-1 and ferritin were products of Santa Cruz Co. (Santa Cruz, CA, USA) and DAKO Ltd. (Glostrup, Denmark), respectively. All other chemicals used were of analytical grade.

Cell cultures

Human epithelial cervical cancer HeLa and epidermoid carcinoma A431 cells were grown in Dulbecco's modified Eagle's medium (DMEM) supplemented with 7% foetal calf serum (FCS) and antibiotics. The cells (1×10^5) in a 1.5-cm-diameter dish were then incubated in the absence or presence of ALA (0.5–1 mM) for 16 h before being exposed to light. Treatment of cells with quinolones was performed for 16–24 h, followed by the addition of ALA to the cell culture (*7*, *8*).

Exposure of the cells to light

The cells were incubated with a specific concentration of ALA for 8–16 h, and 1.0 ml of fresh drug-free medium was then added. Irradiation with visible light was carried out under sterile conditions, using a fluorescence lamp, in a CO_2 incubator. The light was filtered through a glass plate to omit UV light and applied from the bottom of the plate to achieve uniform delivery to the entire plate. The increase of the temperature was confirmed to be <2°C by using a thermo-couple device during exposure to light. The power was calibrated with a power metre, and the period of irradiation was adjusted to obtain fluences of 0.54 J/cm^2. Cell viability was measured by trypan-blue exclusion after trypsinization. The cell activity was also examined by 3-(4,5-dimethyl-thiazol-2-yl)-2,5-diphenyl-2*H*-tetrazolium bromide (MTT) assay. Each experiment was carried out in triplicate or quadruplicate. Controls were as follows: (i) cells exposed to ALA but not exposed to light (dark cytotoxicity), (ii) cells untreated with ALA but exposed to light and (iii) cells exposed to neither ALA nor light. Cell viability (cell survival) was expressed as a percentage of control cells. Porphyrins were extracted from the cells with 96% ethanol containing 0.5 M HCl (*7*). The amount of protoporphyrin was determined by fluorescence spectrophotometry, as previously described (*7*, *17*).

Immunoblotting

The lysates from HeLa cells were subjected to sodium dodecylsulphate-polyacrylamide gel electrophoresis (SDS–PAGE) and electroblotted onto poly(vinylidene difluoride) (PVDF) membrane (Bio-Rad Laboratories, Hercules, CA, USA). Immunoblotting was carried out with antibodies for ferrochelatase, ferritin and transferrin receptor-1 as the primary antibodies (*8*).

Absorption spectra

Ferric chloride (100 μM) was incubated with quinolones (100 μM). Absorption spectra of iron–quinolone complexes were measured using a JASCO V-530 spectrophotometer (Tokyo).

Statistics

Two-sample *t*-tests were used to compare the amount of protoporphyrin and photosensitivity between treated and untreated controls. Comparison of data from different treatment groups was conducted using 1-way analysis of variance (ANOVA). Analysis was performed using Microsoft Excel 2003 software.

Results

Quinolones enhances ALA-induced photodamage

We (*7*, *8*) have previously shown that the ALA-induced accumulation of protoporphyrin is inversely related to the level of ferrochelatase. To obtain a high efficacy of ALA-PDT, the various chemicals affecting the ALA-induced accumulation of protoporphyrin were screened using HeLa cells. The fluorescence pattern with ethanol extracts of the cells treated with 1 mM ALA for 16 h showed a maximum peak at 637 nm with excitation at 400 nm, which was consistent with that of standard protoporphyrin. First, effects of quinolone chemicals, including enoxacin and ciprofloxacin, on the ALA-induced accumulation of protoporphyrin were examined. As shown in Fig. 1A, enoxacin, ciprofloxacin and norfloxacin increased the accumulation of protoporphyrin by incubation of HeLa cells with ALA, in a dose-dependent manner. In the absence of ALA, no accumulation of protoporphyrin in enoxacin- or ciprofloxacin-treated cells was observed. When pre-incubation of cells with enoxacin was carried out, the accumulation increased by 1.4- and 1.9-fold with 16 and 24 h incubation, respectively (Fig. 1B). The pre-treatment with ciprofloxacin, norfloxacin or lomefloxacin was also effective for the accumulation. The growth of cells did not change by the treatment with 100 μM quinolone compounds for 48 h (data not shown). When a concentration of >200 μM these quinolones was used, the accumulation of protoporphyrin gradually declined due to cytotoxicity. To evaluate the effect of enoxacin on ALA-induced photosensitivity of HeLa cells, they were treated with 1 mM ALA for 16 h and then exposed to visible light. The viability of the cells pre-treated with ALA plus 50 and 100 μM

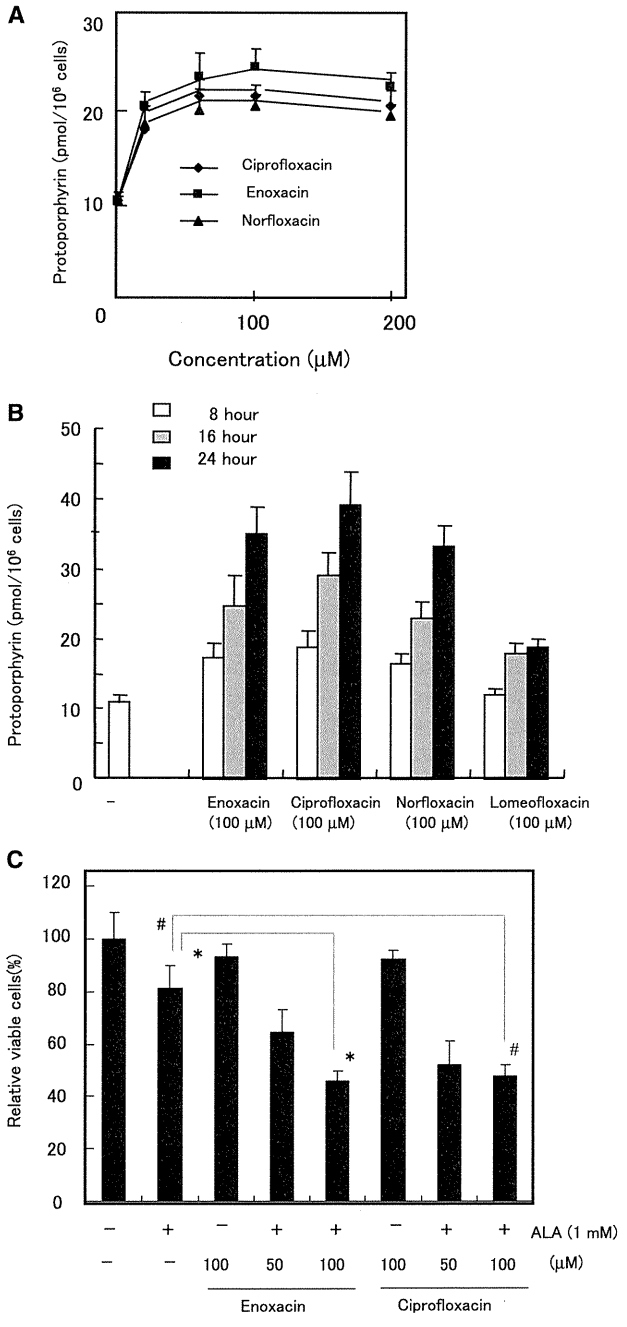

Fig. 1 The increase by quinolone compounds of the accumulation of protoporphyrin and photosensitivity in ALA-treated HeLa cells. (A) Effect of quinolones on the ALA-induced accumulation of protoporphyrin. HeLa cells were incubated with 1 mM ALA plus the indicated concentration of enoxacin, ciprofloxacin or norfloxacin for 16 h. Porphyrin was extracted from the cells and measured using a fluorospectrophotometer. (B) Effect of pre-treatment. HeLa cells were pre-treated with quinolone compounds (100 μM) for the indicated period, and changed to a fresh medium with 1 mM ALA, followed by incubation for 16 h. The concentration of protoporphyrin was determined. (C) Effect of quinolones on ALA-induced photodamage. The cells pre-treated with the indicated concentration of enoxacin or ciprofloxacin for 24 h were incubated without or with 1 mM ALA for 16 h, and then exposed to visible light. Light dose = 0.54 J/cm^2. After trypsinization, the living cells were counted. More than 500 living cells without any treatment were counted. The data are expressed as the average ± SEM for three to four experiments. Two-sample *t*-test was carried out: $^*P<0.005$ and $^\#P<0.005$ versus ALA alone.

enoxacin decreased to 62 and 43%, respectively, which were significantly different compared with that with ALA alone (78%) (Fig. 1C). Ciprofloxacin was also effective for the photodamage. When the cells treated with enoxacin or ciprofloxacin alone were exposed to light, virtually no cell death was observed. No cell death of ALA-treated cells was also observed without exposure to light. In separate experiments, when A431 cells were pre-treated with 100 μM enoxacin, ciprofloxacin or norfloxacin for 24 h, the ALA-induced photodamage was stronger than that with ALA alone (Fig. 2A). In parallel, the ALA-induced accumulation of protoporphyrin in quinolone-treated cells was higher than that in control cells (Fig. 2B). Thus, quinolone compounds such as enoxacin, ciprofloxacin and norfloxacin facilitate ALA-induced photodamage.

The inhibitory effect of haemin and Fe-NTA on ALA-PDT

Figure 3A shows the decrease of the ALA-induced accumulation of protoporphyrin in haemin-treated HeLa cells, suggesting that iron from haem can be reused as the substrate of the ferrochelatase reaction. The addition of Fe-NTA also led to a decrease of the

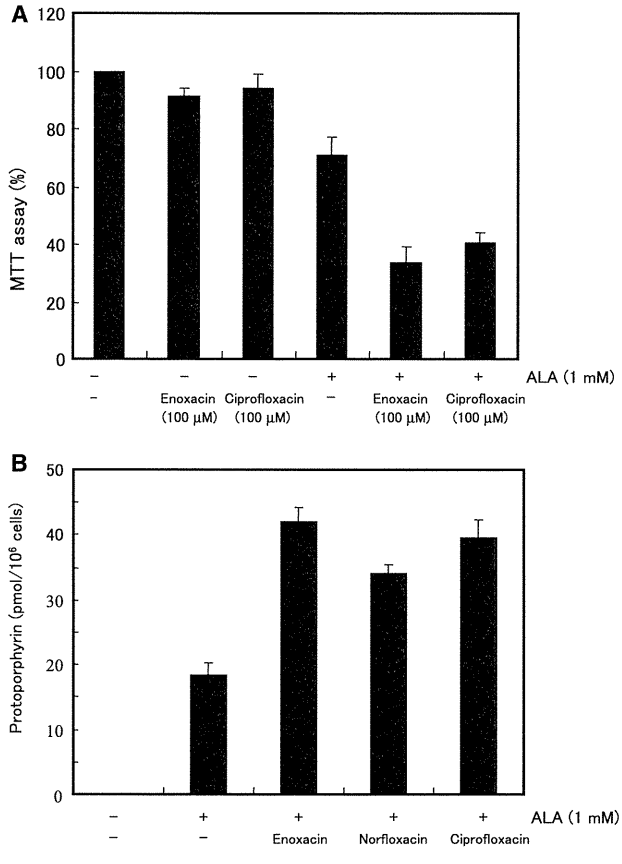

Fig. 2 The increase by enoxacin, norfloxacin or ciprofloxacin of the accumulation of protoporphyrin and photodamage in ALA-treated A431 cells. (A) Treatment of A431 cells with indicated quinolone chemicals (100 μM), in combination with 1 mM ALA. The cells as above were irradiated, and survival of the cells was analysed by the MTT assay. The data are expressed as the average ± SEM for at least three independent experiments. (B) The concentration of protoporphyrin in the cells was determined, similar to those shown in the legend of Fig. 1.

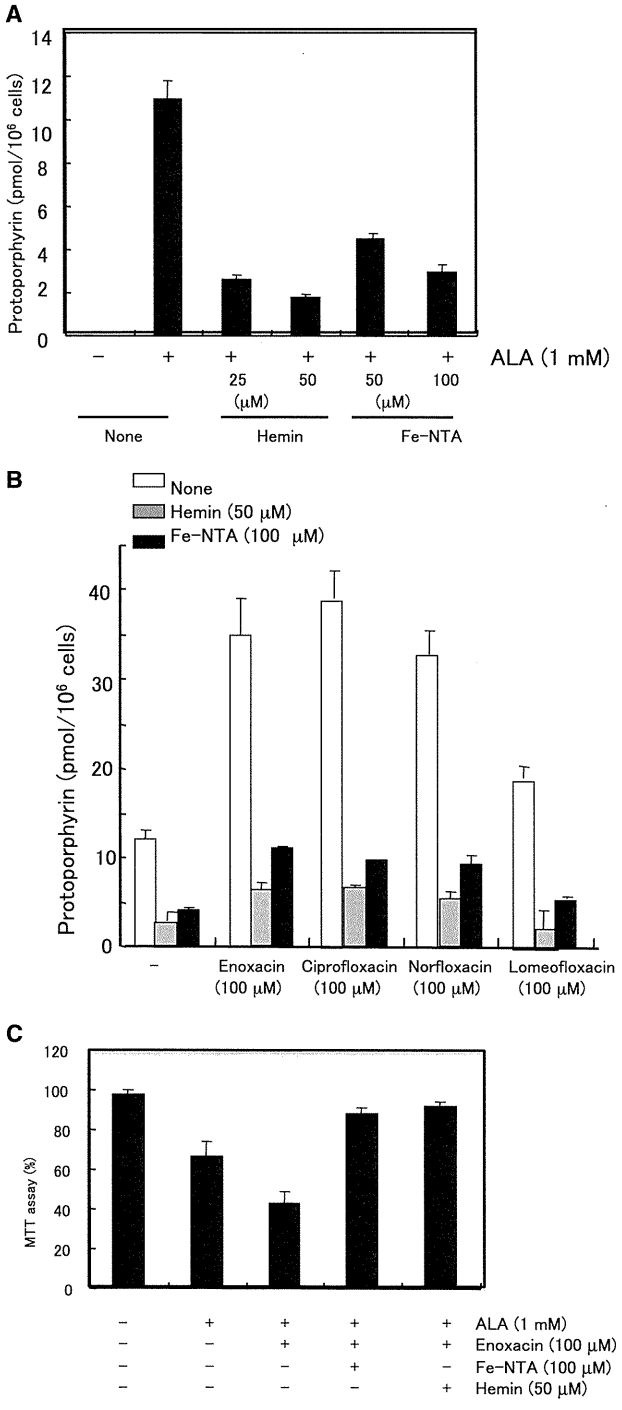

Fig. 3 Effect of haemin and Fe-NTA on ALA-induced accumulation of protoporphyrin and photodamage. (A) The inhibitory effect of haemin and Fe-NTA on the ALA-induced accumulation of protoporphyrin. HeLa cells were incubated with 1 mM ALA plus the indicated concentration of haemin and Fe-NTA for 16 h. Porphyrin was extracted from the cells and measured using a fluorospectrophotometer. (B) Effect of haemin and Fe-NTA on the quinolone-dependent increased accumulation of protoporphyrin. HeLa cells were pre-treated with the indicated concentration of quinolones for 24 h, and then incubated with 1 mM ALA, in combination with haemin or Fe-NTA for 16 h. The accumulated protoporphyrin was measured. (C) Effect of haemin, Fe-NTA and enoxacin on ALA-induced photodamage. The cells pre-treated with enoxacin plus haemin or Fe-NTA as above were irradiated, and survival of the cells was analysed by the MTT assay.

accumulation of protoporphyrin. These results suggest that iron supply for the ferrochelatase reaction is limited in cancerous cells. Then, we examined the effect of haemin or Fe-NTA on the increased accumulation of protoporphyrin by quinolones. As shown in Fig. 3B, enoxacin-, ciprofloxacin-, norfloxacin and lomefloxacin-dependent increases in the accumulation of protoporphyrin were cancelled by the treatment with haemin or Fe-NTA. To evaluate the inhibitory effect of haemin on photosensitivity, the cells treated with enoxacin and haemin were exposed to light. The ALA-induced photodamage in enoxacin-pre-treated HeLa cells was decreased by 50 μM haemin (Fig. 3C). Fe-NTA (100 μM) also reduced the rate of cell death.

Synergistic effect of Sn-protoporphyrin and quinolones on ALA-induced photodamage

We next examined the effect of Sn-protoporphyrin, an inhibitor of haem oxygenase (HO), on ALA-induced accumulation of protoporphyrin. The accumulation was markedly increased in 20 μM Sn-protoporphyrin-treated A431 cells, while the increase was cancelled by co-incubation with 100 μM Fe-NTA and 20 μM Sn-protoporphyrin (Fig. 4A). The addition of 50 μM haemin or 50 μg/ml myoglobin diminished the accumulation in Sn-protoporphyrin-treated cells (Fig. 4A). These results indicated that degradation of haem by HO and subsequent utilization of the released iron for the ferrochelatase reaction contributes to the reduction of the accumulation of protoporphyrin. The photodamage was then evaluated using Sn-protoporphyrin-treated cells. As shown in Fig. 4B, the cell death of Sn-protoporphyrin- and ALA-treated cells was severer than that of ALA-treated cells. Treatment with haemin or Fe-NTA in combination with Sn-protoporphyrin resulted in less photosensitivity. Conversely, pre-treatment of A431 with enoxacin or ciprofloxacin, followed by the treatment with Sn-protoporphyrin and ALA for 16 h led to a marked increase in the photodamage and accumulation of protoporphyrin, as compared with those upon pre-treatment with quinolones alone or treatment with Sn-protoporphyrin alone (Fig. 4C and D). Thus, the use of quinolones plus Sn-protoporphyrin strongly enhances ALA-induced photodamage.

Iron-chelating activity of quinolones

We finally examined the mechanisms involved in the increase in the ALA-induced accumulation of protoporphyrin by quinolones. Figure 5A shows absorption spectra of the iron–quinolone complexes formed by incubation of ferric chloride with an equivalent amount of enoxacin, ciprofloxacin and norfloxacin. Iron–quinolone complexes with visible colours with a maximum at 450 nm were formed, indicating that quinolones function as iron-chelators (*18*). Therefore, to examine changes of cellular metabolism upon quinolone treatments, the levels of iron-metabolizing proteins in enoxacin- or ciprofloxacin-treated cells were analysed by immunoblotting. The level of transferrin receptor-1 in enoxacin- or ciprofloxacin-treated HeLa cells increased compared with that of untreated cells, while ferritin in quinolone-treated cells slightly

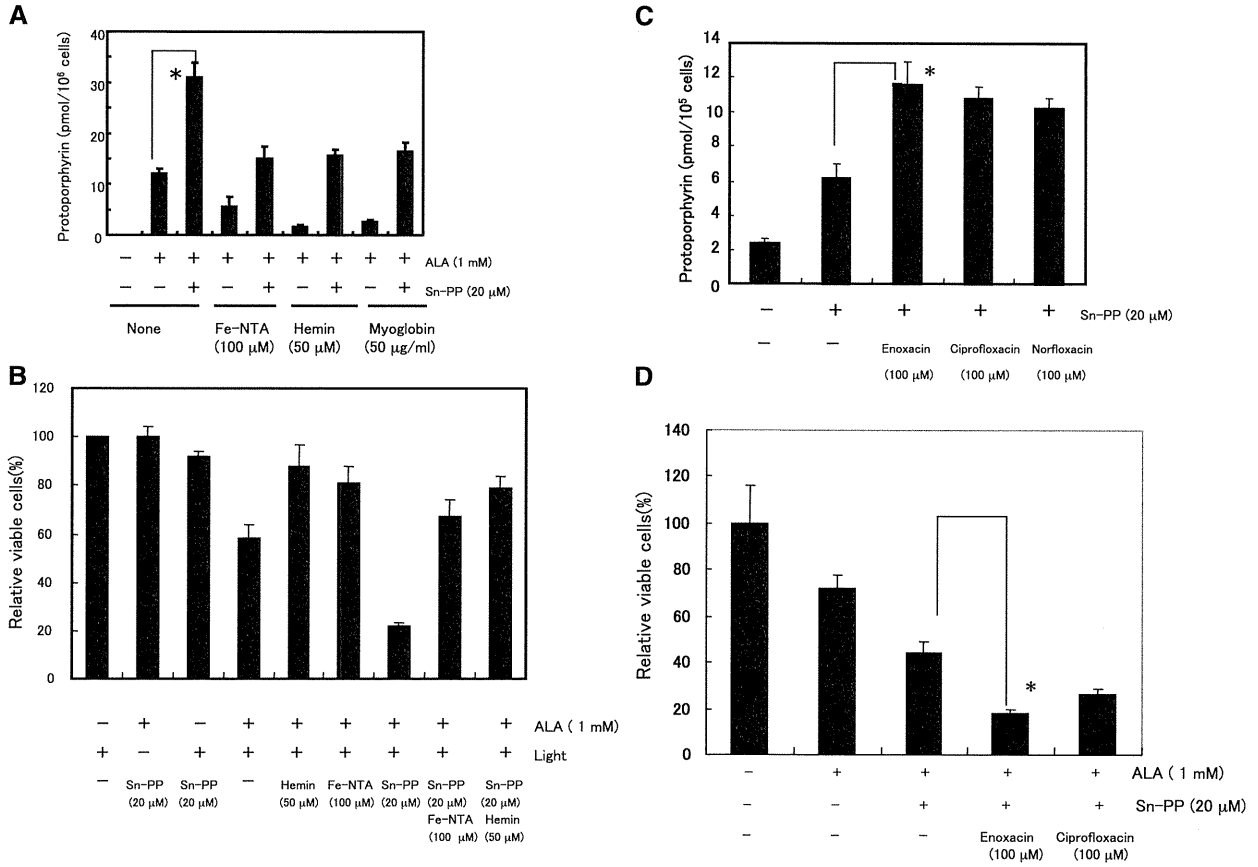

Fig. 4 Effect of Sn-protoporphyrin and quinolone chemicals on ALA-induced accumulation of protoporphyrin and photodamage. (A) Effect of Sn-protoporphyrin on the accumulation of protoporphyrin. A431 cells were incubated with 1 mM ALA in the absence or presence of 20 μM Sn-protoporphyrin (Sn-PP) for 16 h. The indicated cells were simultaneously incubated without or with Fe-NTA, haemin or myoglobin. The concentration of protoporphyrin in the cells was determined. The data are expressed as the average ± SEM for at least three independent experiments. $*P<0.01$. (B) The photosensitivity of the cells. The cells treated as above were exposed to light and the living cells were determined by counting living cells, using trypane blue. More than 500 living cells were counted in control. (C) Effect of quinolones and Sn-protoporphyrin on the accumulation of protoporphyrin. A431 cells were pre-treated with 100 μM enoxacin, 100 μM ciprofloxacin or 100 μM norfloxacin for 24 h, and were incubated with 1 mM ALA in the absence or presence of 20 μM Sn-protoporphyrin (Sn-PP) for 16 h. Protoporphyrin in the cells was examined. The data are expressed as the average ±SEM for three to four independent experiments. $*P<0.005$. (D) The photosensitivity of the cells. The living cells upon exposure to light were measured by the trypane-blue exclusion method. $*P<0.01$.

decreased (Fig. 5B). Since the expression of these proteins changes in a manner dependent on the intracellular level of iron (*19*), quinolones decrease iron utilization in cells. In contrast, virtually no change in the level of ferrochelatase in enoxacin-treated cells was observed although the expression of ferrochelatase was low by the treatment with iron-chelators (*20*), indicating that iron chelation with enoxacin or ciprofloxacin was weak.

Discussion

Since cancer development and progression are highly complex, it is evident that often no single therapeutic modality can be curative. Understanding the cellular and molecular events contributing to PDT-induced apoptosis and recovery from cell death leads to the development of more sophisticated approaches to drug design and therapy. A new molecular-based therapeutics including multiple regimens is more likely to eradicate malignant tissues. The present study first demonstrated that anti-bacterial drugs, quinolones, could enhance the ALA-induced photosensitivity of two kinds of human cancer cells. The effect of quinolones was also seen with colon cancer Colo201 and breast cancer MCF-7 cells. Results based on chemical extraction of porphyrin from cells confirmed the increased production of protoporphyrin upon treatment with quinolones including enoxacin, norfloxacin, ciprofloxacin and lomefloxacin, followed by incubation with ALA. In the absence of exogenously added ALA, neither photodamage nor the accumulation of protoporphyrin was observed even with quinolone-treated cells. The concentration of quinolones up to 100 μM used in this study neither affected cell growth nor showed cytotoxicity. Thus, the treatment of tumour cells with quinolones can enhance efficacy of ALA-induced photodamage.

We (*7*) previously reported that desferrioxamine, an iron-chelator, markedly enhanced ALA-induced photosensitivity *in vitro*. Quinolones act as chelating agents with metal ions such as calcium and magnesium (*21*, *22*). We showed the formation of enoxacin-, norfloxacin- and ciprofloxacin-iron complexes by determining absorption spectra (Fig. 5A), indicating that chelation of iron with quinolones occurred. This

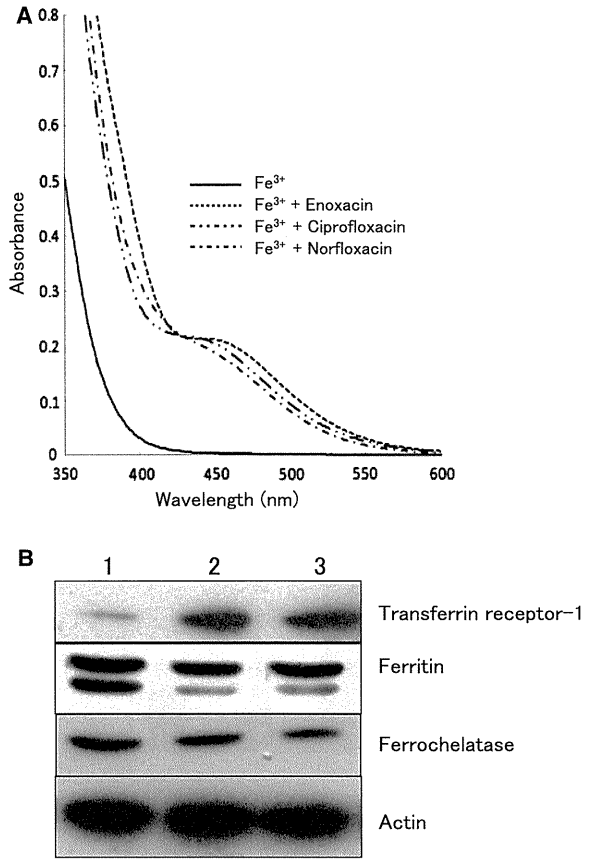

Fig. 5 Quinolone chemicals chelate with iron and affect the expression of iron-metabolizing proteins. (A) Spectroscopic scan of quinolone chemicals complexed with ferric ion. Ferric chloride (100 μM) was incubated without or with 100 μM enoxacin, 100 μM ciprofloxacin or 100 μM norfloxacin in phosphate-buffered saline at room temperature for 5 min. Absorption spectra of the formed iron–quinolone complexes were measured. Lower scan is a comparison of ferric chloride without quinolones. (B) Immunoblot analysis of transferrin receptor-1, ferritin and ferrochelatase in enoxacin- or ciprofloxacin-treated HeLa cells. The cells were treated without (lane 1) or with 100 μM enoxacin (lane 2) or 100 μM ciprofloxacin (lane 3) for 24 h, washed twice with phosphate-buffered saline, and then lysed. The cellular proteins were analysed by SDS-PAGE, and immunoblotting was performed using antibodies for transferrin receptor-1, ferritin, ferrochelatase and actin, as the primary antibodies.

observation was similar to that seen in case of desferrioxamine-iron complex (*23*). Immunoblot analysis revealed that the expression of transferrin receptor-1 was high and that of ferritin was low in enoxacin- and ciprofloxacin-treated cells compared with those of untreated cells. On the Basis of the fact that the alteration of expressions of both proteins occurs in a manner dependent on the level of intracellular iron (*19*), the treatment of cells with quinolones leads to iron deficiency. We (*20*) previously found that ferrochelatase is an iron-sulphur-containing enzyme and its expression was markedly decreased in iron-deficient cells. The decrease of the level of ferrochelatase was essential for ALA-PDT (*7*, *8*). The present data showed that the expression of ferrochelatase in enoxacin- and ciprofloxacin-treated cells was basically unchanged. Moreover, neither enoxacin nor ciprofloxacin inhibited iron-chelating ferrochelatase activity (Y. Ohgari & S. Taketani, unpublished results), suggesting that the iron deficiency in cells by the treatment with quinolones can be weak. Therefore, since the utilization of iron for ferrochelatase reaction *in vivo* is liable to drop by the treatment with quinolones, it is possible that the accumulation of protoporphyrin is, in contrast, increased.

We (*7*) previously reported that the low level of ferrochelatase in tumour cells could contribute to the ALA-induced accumulation of protoporphyrin and subsequent photodamage *in vitro*. The production of NO increased the ALA-induced photodamage by decreasing the levels of mitochondrial iron-containing enzymes including ferrochelatase and NADH dehydrogenase (*8*). Furthermore, the irradiation of epidermal cells led to a decrease of the level of ferrochelatase, which is mediated by the generation of reactive oxygen species (*24*). Thus, the ferrochelatase reaction is deeply related to mitochondrial functions. The present study showed that the level of ferrochelatase in enoxacin- or ciprofloxacin-treated cells was not decreased since these chemicals showed low cytotoxicity and caused partial iron deficiency. However, it is possible that quinolones target some unidentified proteins in mitochondria, which are related to iron metabolism, and then the utilization of iron to haem biosynthesis can be down-regulated.

In addition of the enhancement of *in vitro* ALA-induced photodamage by quinolones, we showed that Sn-protoporphyrin, an inhibitor of HO (*25*), increased the ALA-induced accumulation of protoporphyrin and photosensitivity. In humans, two isoforms of HO have been characterized: a constitutive expressed form, HO-2, and an inducible form, HO-1. The reduced expression of HO-1 mRNA by siRNA increased cell death upon ALA-PDT (*26*). Therefore, the decrease of HO function can contribute to the ALA-induced accumulation of protoporphyrin. We have showed that HO-1 is markedly induced not only by agents and chemicals that produce oxidative stress involving the generation of reactive oxygen species but also by the substrate haem (*27*, *28*). Then, through ALA-induced photodamage, HO-1 in ALA-treated cells was induced in time- and dose-dependent manners, and the induction of HO-1 was seen in the protoporphyrin-accumulated cells (*7*). It is considered that uncommitted haem in the cells is very dangerous for the maintenance of living systems, and reutilization of iron, including degradation of the haem, catalysed by HO, is essential for the homeostasis of iron in cells (*19*). Then, excess haem produced from ALA may induce HO-1. It was also considered possible that the accumulated protoporphyrin may generate reactive oxygen species via autoxidation (*29*), which leads to the induction of HO-1. This possibility was ruled out by the observations that the increased accumulation of protoporphyrin by Sn-protoporphyrin was cancelled by the exogenously added haemin or Fe-NTA. On the other hand, on the basis of the fact that HO degrades haem, producing iron, CO and biliverdin (*20*), the supply of iron for its reutilization is stopped by the inhibition of the HO reaction with Sn-protoporphyrin, leading to the increase in the

production of protoporphyrin. The present data revealed that enoxacin and Sn-protoporphyrin in combination exhibited a synergistic effect on ALA-induced accumulation of protoporphyrin as well as photodamage. Not only the decrease of reutilization of iron by HO but also the decrease of the utilization of mitochondrial iron for haem biosynthesis can further promote ALA-PDT. Nevertheless, it is still possible that there are other effects of quinolones on cellular metabolism.

Quinolones target several kinds of bacterial topoisomerases, resulting in inhibition of DNA synthesis (*13*, *14*), but several types of quinolones exhibit negative side effects, including significant phototoxicity (*30*). Quinolone-dependent phototoxicity is probably not due to the accumulation of protoporphyrin but instead to the generation of phototoxic metabolites of the drugs in cells, leading to DNA fragmentation and modification (*31*). The present data show that the augmentation of ALA-induced photodamage by quinolones is not responsible for the phototoxicity of quinolones, since the sole treatment with 100 μM enoxacin, ciprofloxacin or norfloxacin did not show photosensitivity because of the low concentration of drugs as well as a low dose of light (Fig. 1C). In addition, it is possible the phototoxicity of quinolones may be helpful to further augment the efficacy of ALA-PDT.

Quinolones were chosen as an attractive candidate agent for PDT because quinolones are widely used in clinical contexts, show relatively low toxicity (*13*), and can be easily administered orally with large volume of distribution and good tissue penetration (*14*). The concentration of quinolones used in this study was equivalent to that in blood of patients (10–250 μM) by clinically conventional therapy (*32*). These properties of quinolones are safer than those of iron-chelators including desferrioxamine. Other studies have recently shown their anti-tumour activity in a variety of human tumour cells by inhibiting the proliferation of tumour cells and promoting apoptosis (*33*, *34*). Furthermore, very recently, quinolone compounds were shown to enhance RNAi by interacting with trans-activating responsive region RNA-binding protein and may be useful as RNAi enhancers in the development of research tools and therapeutics (*35*). Taken together, the application of anti-bacterial agents, quinolones, may be extremely effective for ALA-PDT and their use in multiple combinations with other therapeutic reagents can optimize the treatment modalities for PDT of various tumour tissues.

Acknowledgements

The authors thank Ms Asami Itoh, Ms Taeko Miyagi and Ms Saki Gotoh for their expert technical assistance.

Funding
Ministry of Education, Culture, Sports, Science and Technology of Japan; Japan Science and Technology Agency.

Conflict of interest
None declared.

References

1. Dougherty, T.J., Gomer, C.J., Henderson, B.W., Jori, G., Kessel, D., Korbelik, M., Moan, J., and Peng, Q. (2004) Photodynamic therapy. *J. Natl Cancer Inst.* **90**, 889–905
2. Chen, Y., Zheng, X., Dobhal, M.D., Gryshuk, A., Morgan, J., Dougherty, T.J., Oseroff, A., and Pandey, P.K. (2005) Methyl pyropheophorbide-a analogues: potential fluorescent probes for the peripheral-type benzodiazepine receptor. Effect of central metal in photosensitizing efficacy. *J. Med. Chem.* **48**, 3692–3695
3. De Rosa, F.S., Lopez, R.F., Thomazine, J.A., Tedesco, A.C., Lange, N., and Bentley, M.V. (2004) In vitro metabolism of 5-ALA esters derivatives in hairless mice skin homogenate and in vivo PpIX accumulation studies. *Pharm. Res.* **21**, 2247–2252
4. Fischer, F., Dickson, E.F., Kennedy, J.C., and Pottier, R.H. (2001) An affordable, portable fluorescence imaging device for skin lesion detection using a dual wavelength approach for image contrast enhancement and aminolaevulinic acid-induced protoporphyrin IX. Part II. In vivo testing. *Lasers Med. Sci.* **16**, 207–212
5. Peng, Q., Berg, K., Moan, J., Kongshaug, M., and Nesland, J.M. (1997) 5-Aminolevulinic acid-based photodynamic therapy: principles and experimental research. *Photochem. Photobiol.* **65**, 235–251
6. Peng, Q., Warloe, T., Berg, K., Moan, J., Kongshaug, M., Giercksky, K.E., and Nesland, J.M. (1997) 5-Aminolevulinic acid-based photodynamic therapy. Clinical research and future challenges. *Cancer* **79**, 2282–2308
7. Ohgari, Y., Nakayasu, Y., Kitajima, S., Sawamoto, M., Mori, H., Shimokawa, O., Matsui, H., and Taketani, S. (2005) Mechanisms involved in delta-aminolevulinic acid (ALA)-induced photosensitivity of tumor cells: relation of ferrochelatase and uptake of ALA to the accumulation of protoporphyrin. *Biochem. Pharmacol.* **71**, 42–49
8. Yamamoto, F., Ohgari, Y., Yamaki, N., Kitajima, S., Shimokawa, O., Matsui, H., and Taketani, S. (2007) The role of nitric oxide in delta-aminolevulinic acid (ALA)-induced photosensitivity of cancerous cells. *Biochem. Biophys. Res. Commun.* **353**, 541–546
9. Lim, H.W. and Cooper, K. (1999) The health impact of solar radiation and prevention strategies: report of the environment council, American academy of dermatology. *J. Am. Acad. Dermatol.* **41**, 81–99
10. Madan, V., Lear, J.T., and Szeimies, R.M. (2010) Non-melanoma skin cancer. *Lancet* **375**, 673–685
11. Fink-Puches, R., Soyer, H.P., Hofer, A., Kerl, H., and Wolf, P. (1998) Long-term follow-up and histological changes of superficial nonmelanoma skin cancers treated with topical delta-aminolevulinic acid photodynamic therapy. *Arch. Dermatol.* **134**, 821–826
12. Adam, H.J., Hoban, D.J., Gin, A.S., and Zhanel, G.G. (2009) Association between fluoroquinolone usage and a dramatic rise in ciprofloxacin-resistant Streptococcus pneumoniae in Canada, 1997–2006. *Int. J. Antimicrob. Agents* **34**, 82–85
13. Drlica, K. and Zhao, X. (1997) DNA gyrase, topoisomerase IV, and the 4-quinolones. *Microbiol. Mol. Biol. Rev.* **61**, 377–392
14. Hooper, D.C. (2000) Mechanisms of action and resistance of older and newer fluoroquinolones. *Clin Infect Dis.* **31 (Suppl. 2)**, S24–S28
15. Herold, C., Ocker, M., Ganslmayer, M., Gerauer, H., Hahn, E.G., and Schuppan, D. (2003) Ciprofloxacin induces apoptosis and inhibits proliferation of human colorectal carcinoma cells. *Br. J. Cancer* **86**, 443–448

16. Taketani, S., Kakimoto, K., Ueta, H., Masaki, R., and Furukawa, T. (2003) Involvement of ABC7 in the biosynthesis of heme in erythroid cells: interaction of ABC7 with ferrochelatase. *Blood* **101**, 3274–3280
17. Tahara, T., Sun, J., Nakanishi, K., Yamamoto, M., Mori, H., Saito, T., Fujita, H., Igarashi, K., and Taketani, S. (2004) Heme positively regulates the expression of beta-globin at the locus control region via the transcriptional factor Bach1 in erythroid cells. *J. Biol. Chem.* **279**, 5480–5487
18. Eboka, C.J., Aigbavboa, S.O., and Akerele, J.O. (1997) Colorimetric determination of the fluoroquinolones. *J. Antimicrob. Chemother.* **39**, 639–641
19. Taketani, S. (2005) Aquisition, mobilization and utilization of cellular iron and heme: endless findings and growing evidence of tight regulation. *Tohoku J. Exp. Med.* **205**, 297–318
20. Taketani, S., Adachi, Y., and Nakahashi, Y. (2000) Regulation of the expression of human ferrochelatase by intracellular iron levels. *Eur. J. Biochem.* **267**, 4685–4692
21. Polk, R.E. (1989) Drug-drug interactions with ciprofloxacin and other fluoroquinolones. *Am. J. Med.* **87**, 76S–81S
22. Teixeira, M.H., Vilas-Boas, L.F., Gil, V.M., and Teixeira, F. (1995) Complexes of ciprofloxacin with metal ions contained in antacid drugs. *J. Chemother.* **7**, 126–132
23. Cramer, S.M., Nathanael, B., and Horváth, C. (1984) High-performance liquid chromatography of deferoxamine and ferrioxamine: interference by iron present in the chromatographic system. *J. Chromatogr.* **295**, 405–411
24. He, D., Behar, S., Nomura, N., Sassa, S., Taketani, S., and Lim, H.W. (1995) The effect of porphyrin and radiation on ferrochelatase and 5-aminolevulinic acid synthase in epidermal cells. *Photodermatol. Photoimmunol. Photomed.* **11**, 25–30
25. Landaw, S.A., Sassa, S., Drummond, G.S., and Kappas, A. (1987) Proof that Sn-protoporphyrin inhibits the enzymatic catabolism of heme in vivo. Suppression of 14CO generation from radiolabeled endogenous and exogenous heme sources. *J. Exp. Med.* **165**, 1195–1200
26. Frank, J., Lornejad-Schäfer, M.R., Schöffl, H., Flaccus, A., Lambert, C., and Biesalski, H.K. (2007) Inhibition of heme oxygenase-1 increases responsiveness of melanoma cells to ALA-based photodynamic therapy. *Int. J. Oncol.* **31**, 1539–1545
27. Masuya, Y., Hioki, K., Tokunaga, R., and Taketani, S. (1998) Involvement of the tyrosine phosphorylation pathway in induction of human heme oxygenase-1 by hemin, sodium arsenite, and cadmium chloride. *J. Biochem.* **124**, 628–633
28. Andoh, Y., Mizutani, A., Ohashi, T., Kojo, S., Ishii, T., Adachi, Y., Ikehara, S., and Taketani, S. (2006) The antioxidant role of a reagent, 2′,7′-dichlorodihydrofluorescin diacetate, detecting reactive-oxygen species and blocking the induction of heme oxygenase-1 and preventing cytotoxicity. *J. Biochem.* **140**, 483–489
29. Ryter, S.W. and Tyrrell, R.M. (2000) The heme synthesis and degradation pathways: role in oxidant sensitivity. Heme oxygenase has both pro- and antioxidant properties. *Free Radic. Biol. Med.* **28**, 289–309
30. Agrawal, N., Ray, R.S., Farooq, M., Pant, A.B., and Hans, P.K. (2007) Photosensitizing potential of ciprofloxacin at ambient level of UV radiation. *Photochem. Photobiol.* **83**, 1226–1236
31. Hemeryck, A., Mamidi, R.N., Bottacini, M., Macpherson, D., Kao, M., and Kelley, M.F. (2006) Pharmacokinetics, metabolism, excretion and plasma protein binding of 14C-levofloxacin after a single oral administration in the Rhesus monkey. *Xenobiotica* **36**, 597–613
32. Thompson, A.M. (2007) Ocular toxicity of fluoroquinolones. *Clin. Experiment. Ophthalmol.* **35**, 566–577
33. Pommier, Y., Leo, E., Zhang, H., and Marchand, C. (2010) DNA topoisomerases and their poisoning by anticancer and antibacterial drugs. *Chem. Biol.* **17**, 421–433
34. El-Rayes, B.F., Grignon, R., Aslam, N., Aranha, O., and Sarkar, F.H. (2002) Ciprofloxacin inhibits cell growth and synergises the effect of etoposide in hormone resistant prostate cancer cells. *Int. J. Oncol.* **21**, 207–211
35. Shan, G., Li, Y., Zhang, J., Li, W., Szulwach, K.E., Duan, R., Faghihi, M.A., Khalil, A.M., Lu, L., Paroo, Z., Chan, A.W., Shi, Z., Liu, Q., Wahlestedt, C., He, C., and Jin, P. (2008) A small molecule enhances RNA interference and promotes microRNA processing. *Nat. Biotechnol.* **26**, 933–940

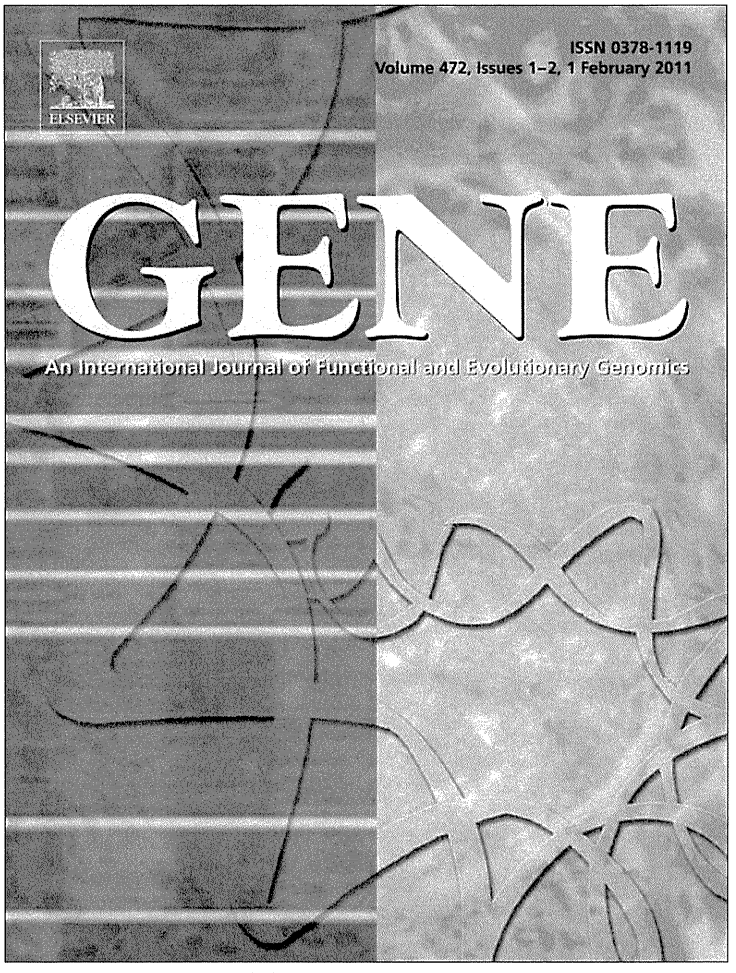

Gene 472 (2011) 28–36

Contents lists available at ScienceDirect

Gene

journal homepage: www.elsevier.com/locate/gene

Egr-1 regulates the transcriptional repression of mouse δ-aminolevulinic acid synthase 1 by heme

Saki Gotoh [a], Takayuki Nakamura [a], Takao Kataoka [a], Shigeru Taketani [a,b,*]

[a] Department of Biotechnology, Kyoto Institute of Technology, Sakyo-ku, Kyoto 606-8585, Japan
[b] Insect Biomedical Center, Kyoto Institute of Technology, Sakyo-ku, Kyoto 606-8585, Japan

ARTICLE INFO

Article history:
Accepted 22 October 2010
Available online 29 October 2010

Received by A. Rynditch

Keywords:
δ-aminolevulinic acid synthase
Repression
Egr-1
NAB1/2
Heme

ABSTRACT

δ-Aminolevulinic acid synthase 1 (ALAS1) is the first and rate-limiting enzyme in the heme biosynthesis. It has been well known that heme exerts a negative feedback control over the transcription of *ALAS1* gene to maintain intracellular heme at appropriate level. To clarify the mechanisms by which heme regulates the expression of ALAS1, we examined the promoter activity of the gene and identified the heme-responsive element (HRE) located in the proximal promoter of the mouse *ALAS1* gene. Reporter and EMSA assays revealed the sequence (GCGGGGGCG), as the site of repression by heme, at −301/−293 bp of the ALAS1 promoter. Subsequently, EMSA and ChIP assays showed that a transcription factor, early growth response 1 (Egr-1) and its major corepressors, NAB1 and NAB2 were found to bind to the ALAS1-HRE, and these bindings increased dependent on the level of intracellular heme. When Egr-1 and NAB1 in combination were expressed in the cells, decreases of the level of ALAS1 mRNA and intracellular level of heme were observed. These results suggest that Egr-1–NABs complex is involved in the regulation of the transcription of ALAS1 by heme, leading to the regulation of the heme biosynthesis.

1. Introduction

Heme biosynthesis in eukaryotic cells is composed of eight enzymatic steps, of which the first and the last three steps take place in the mitochondria, whereas the others in the cytoplasm. ALAS is the first and rate-limiting enzyme in the heme biosynthesis (Sassa, 1988). There are two isozymes for ALAS, namely, ALAS1 and ALAS2, encoded by separate genes. ALAS1 is ubiquitously expressed and provides heme for cytochromes and other hemoproteins (Furuyama et al., 2007). ALAS2 is expressed exclusively in erythroid cells and synthesizes heme specifically for hemoglobin (Kramer et al., 2000). It has been well known that heme negatively regulates ALAS1 expression by feedback mechanisms including reduction of transcription and translation, destabilization of mRNA and inhibition of mitochondrial transport of precursor protein, and it plays a crucial role for maintaining intracellular heme at appropriate level (Schuurmans et al., 2001; Furuyama et al., 2007). It is shown that PGC-1α via an insulin sensitive FOXO1 site within the promoter of ALAS1 can be involved in fasting response to the induction of ALAS1 (Handschin et al., 2005). The PGC-1α dependent transcriptional activity of ALAS1 gene seems to be reduced by a nuclear receptor Rev-erbα and β when heme binds to Rev-erbs after which recruit the corepressor NcoR (Yin et al., 2007; Wu et al., 2009). On the other hand, it is also shown that the circadian expression of ALAS1 can be controlled by the clock factor NPAS2–BMAL1 complex, which is regulated in a CO-heme-dependent manner (Kaasik and Lee, 2004). Thus various transcription factors are involved in transcriptional regulation of ALAS1 gene to various stimuli, but it is not still fully clarified how heme is involved in the transcriptional repression.

Egr-1 is a member of early growth response transcription factors that belong to immediately early genes that trigger de novo transcription of external stimuli (Svaren et al., 1996; Khachigian, 2006). Egr-1 binds to a GC-rich promoter motif to regulate the expression of various gene family including growth factor, cytokines and transcription factors (Blaschke et al., 2004). In contrast to the universal and immediate response of Egr-1 to mitogenic factors, Egr-1 also exhibits the suppressive gene activity via binding to or transactivation of major suppressor factors (Gashler et al., 1993; Svaren et al., 1996). This includes the interaction of Egr-1 with NAB1 and NAB2 transcriptional corepressors, whose complex deeply represses the activation of their target promoters (Blaschke et al., 2004; Kumbrink et al., 2005). Egr-1 is readily up-regulated by ischemia/reperfusion, hypoxia, hyperoxia and hemorrhagic shock, all inducers of ROS-mediated signaling and inflammation. Oxidative stress derived from heme in vascular smooth muscle cells caused the marked induction of Egr-1 expression (Hasan and Schafer, 2008;

Abbreviations: ALAS, δ-aminolevulinate synthase; PGC-1α, peroxisome proliferator-activated receptor γ coactivator 1 α; DMEM, Dulbecco's modified Eagle's medium; FCS, fetal calf serum; SA, succinylacetone; HRE, heme-responsive element; RT, reverse transcriptase; EMSA, electrophoretic mobility shift assays; Egr-1, early growth response 1; SDS-PAGE, sodium dodecylsulfate-polyacrylamide gel electrophoresis; NAB1/2, NGFI-A binding proteins 1/2; ChIP, chromatin immunoprecipitation.

* Corresponding author. Department of Biotechnology, Kyoto Institute of Technology, Sakyo-ku, Kyoto 606-8585, Japan. Tel./fax: +81 75 724 7789.
E-mail address: taketani@kit.ac.jp (S. Taketani).

0378-1119/$ – see front matter © 2010 Elsevier B.V. All rights reserved.
doi:10.1016/j.gene.2010.10.008

Rokosh, 2008), which may relate to cellular effects by increasing intracellular level of heme.

We tried to clarify the precise mechanism by which heme represses the transcription of the mouse *ALAS1* gene. Here we show the identification of a HRE in the mouse *ALAS1* gene promoter that is responsible for the repression by Egr-1 and its corepressors NAB1/2. Thus, Egr-1 complex newly functions as a heme-inducible repressor for the mouse *ALAS1* gene.

2. Materials and methods

2.1. Materials

[γ-^{32}P] ATP and poly (dI-dC) were purchased from GE Biosciences Co. (Buckinghamshire, UK). Restriction endonucleases and DNA modifying enzymes were obtained from Takara Co. (Kyoto, Japan) and Toyobo Co. (Tokyo Japan), respectively. The transfection reagent Hilymax was from Dojin Co. Ltd, (Tokyo, Japan). Antibodies for Egr-1, NAB1, NAB2 and actin were purchased from Santa Cruz Biotechnoloy Inc. (Santa Cruz, CA). All other chemicals were of analytical grade.

2.2. Cell cultures and treatment

Mouse embryonic fibroblast NIH3T3 and mouse hepatoma Hepa1-6 cells were grown in DMEM supplemented with 7% FCS and antibiotics. The cells were treated for 4–16 h in the medium supplemented with 7% FCS containing 10–50 μM hemin or 1 mM SA.

2.3. Plasmids

To construct the luciferase reporter plasmid with the *ALAS1* gene promoter, ALAS1 promoter region (−1241 to +39) was amplified by PCR using the sense primer (5'-TGATGATTTGGGTCAGG-3') and the antisense primer (5'-AACTCGAGCGGAGGACGCT-3'). The template named pANH III carrying the mouse *ALAS1* gene was a kind gift of Dr. O. Nakajima (Okano et al., 2010). Amplified DNA fragment was subcloned into *Sac*I/*Xho*I-digested pGL3B (Promega), named as pGL-ALAS1p.

Reporter plasmid pGL-ALAS1(−302), pGL-ALAS1(−297), pGL-ALAS1(−293) and pGL-ALAS1(−62) were made as follows: PCR amplification was performed with antisense primer (5'-AAAA-GCTTCTCGAGCGGAGGACGCT-3') and the following sense primers

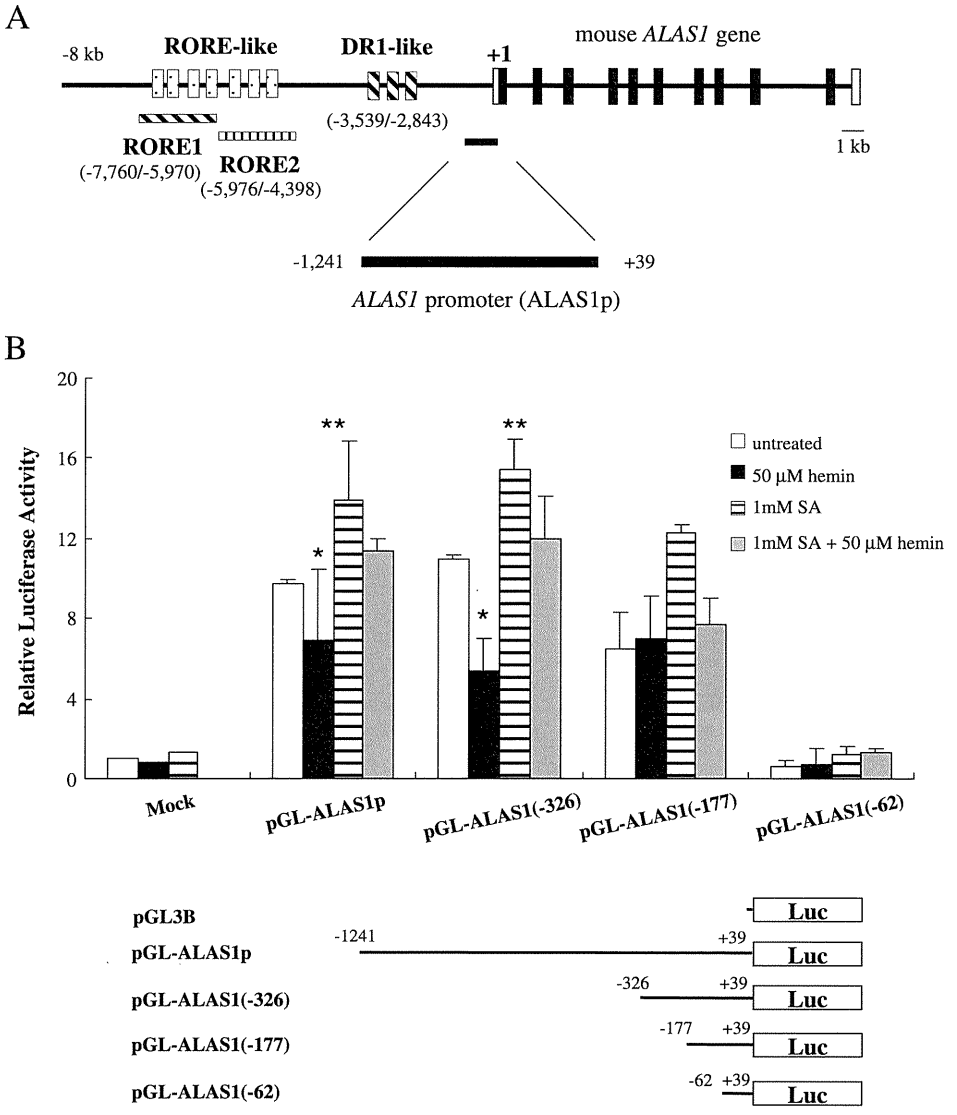

Fig. 1. Repression of the transcriptional activity of the mouse ALAS1 promoter region by heme. (A) Schematic representation of 5'-flanking region of the mouse *ALAS1* gene. (B) Effect of hemin and SA on the transcriptional activity of the mouse ALAS1 promoter. NIH3T3 cells were transiently transfected with pGL-ALAS1p, pGL-ALAS1 (−326), pGL-ALAS1 (−177) or pGL-ALAS1 (−62), followed by the treatment with 50 μM hemin and/or 1 mM SA for 16 h. Luciferase activity was measured and normalized to *Renilla* luciferase activity. The data are the average ± SEM for at least three independent experiments (*$P<0.05$, hemin treatment versus vehicle control; **$P<0.01$, SA treatment versus control).

(5'-AAGAGCTCAGCGGGGGCGCAGGAGT-3') for pGL-ALAS1(−302), (5'-AAGAGCTCGGGCGCAGGAGTCTGAC-3') for pGL-ALAS1(−297), (5'-AAGAGCTCGCAGGAGTCTGACGCAT-3') for pGL-ALAS1(−293), and (5'-AAGAGCTCCGCGGCGGTCACTCCGGC-3') for pGL-ALAS1(−62). Amplified fragments were subcloned into *Sac*I/*Hind*III-digested pGL3B. To construct pGL-ALAS1(−326) and pGL-ALAS1(-177), pGL-ALAS1p was digested with *Sma*I or *Aat*I/*Sma*I, the resulting fragments were self-ligated, and named as pGL-ALAS1(−326) and pGL-ALAS1(-177). pGL-ALAS1(−302)mtA and pGL-ALAS1(−302)mtB were made by PCR using the antisense primer (5'-AAAAGCTTCTCGAGCGGAG-GACGCT-3') plus the following mutagenic sense primers (5'-AAGAGCTCAGTGGGGGCGCAGGAGT-3') for mtA, and (5'-AAGAGCT-CAGCGTGGGCGCAGGAGT-3') for mtB. Amplified fragments were subcloned into *Sac*I/*Hind*III-digested pGL3B.

The reporter plasmids containing minimal promoter, pALAS1 HRE (×2) and pALAS1 HRE (×4) were constructed as follows: Double strand oligonucleotides containing ALAS1 HRE (5'-GCGG-GGGCGAATTTGCGGGGGCGTCA-3') were phosphorylated, and ligated into each other then to the *Pst*I site of pBluescript K/S$^+$. The clones with two and four tandem repeat of the consensus HRE were selected, the

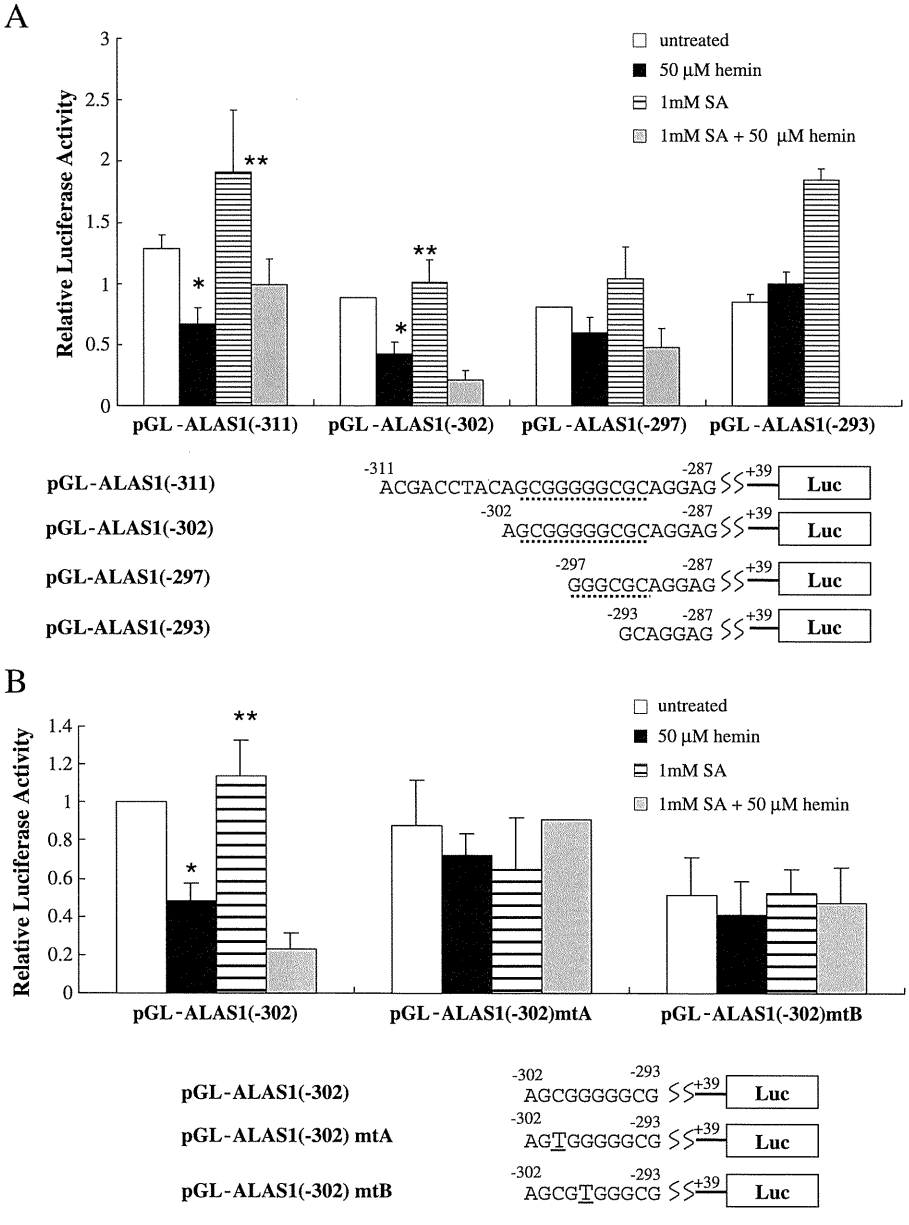

Fig. 2. Characterization of HRE in the mouse ALAS1 promoter. (A) Reporter activity of the mouse ALAS1 promoter in hemin- and SA-treated NIH3T3 cells. The cells were transfected with pGL-ALAS1 (−311), pGL-ALAS1 (−302), pGL-ALAS1 (−297), pGL-ALAS1 (−293), followed by the treatment with 50 μM hemin and/or 1 mM SA. Luciferase activity was measured and normalized to *Renilla* luciferase activity. The data are the average ± SEM for at least three independent experiments (*P<0.01, hemin treatment versus vehicle control; **P<0.05, SA treatment versus control). (B) Effect of mutations in the ALAS1-HRE on the transcriptional activity in hemin- and SA-treated NIH3T3 cells. Mutations in ALAS1-HRE were generated by site-directed mutagenesis. NIH3T3 cells were transfected with the indicated mutated constructs. The cells were treated without or with 50 μM hemin and/or 1 mM SA for 16 h. Luciferase activity was measured and normalized to *Renilla* luciferase activity. The data are the average ± SEM for at least three independent experiments (*P<0.01, hemin treatment versus vehicle control; **P<0.05, SA treatment versus control). (C) The reporter activity of the ALAS1-HRE. NIH3T3 cells were transfected with the ALAS1-HRE constructs as indicated. The cells were treated without or with 50 μM hemin and/or 1 mM SA for 16 h. Luciferase activity was measured and normalized to *Renilla* luciferase activity. The data are the average ± SEM of at least three independent experiments (*P<0.005, hemin treatment versus untreated control; **P<0.01, SA treatment versus untreated control). (D) EMSA of oligonucleotides containing the ALAS1-HRE with mutated competitors. EMSA was performed with nuclear extracts from untreated Hepa1-6 cells using ^{32}P-labeled ALAS1-HRE. Competitive assay was carried out by the addition of a 50-fold excess amount of mutated ALAS1-HRE oligonucleotides. An arrow indicates the position of a major competitive band. (E) ALAS1-HRE homologues found in the ALAS1 promoters of mouse, rat and human.

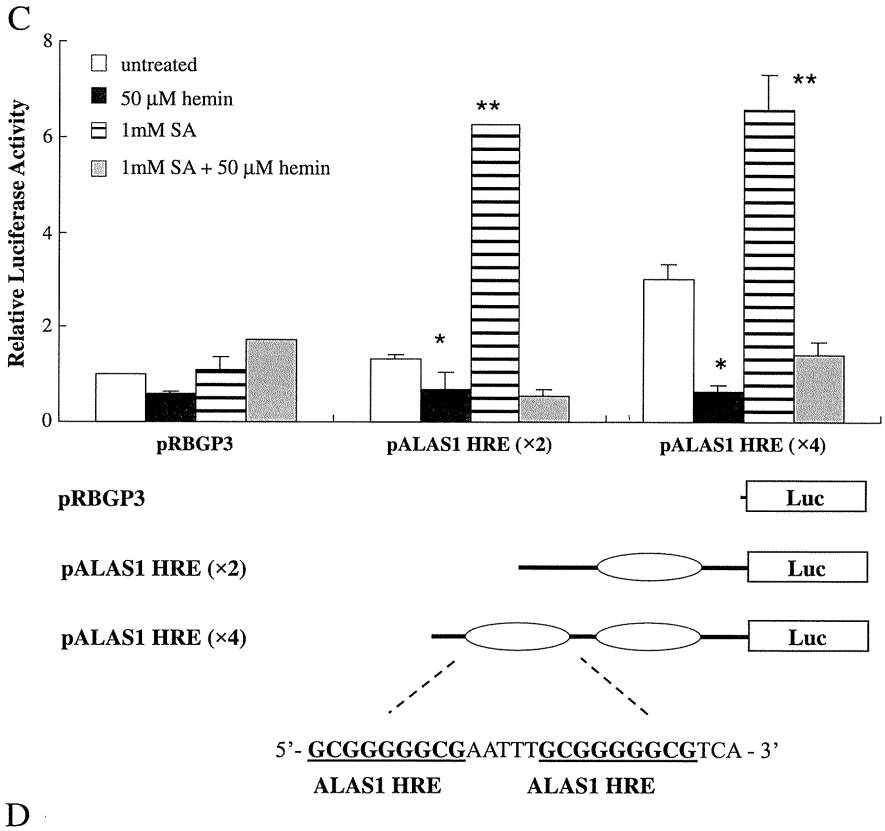

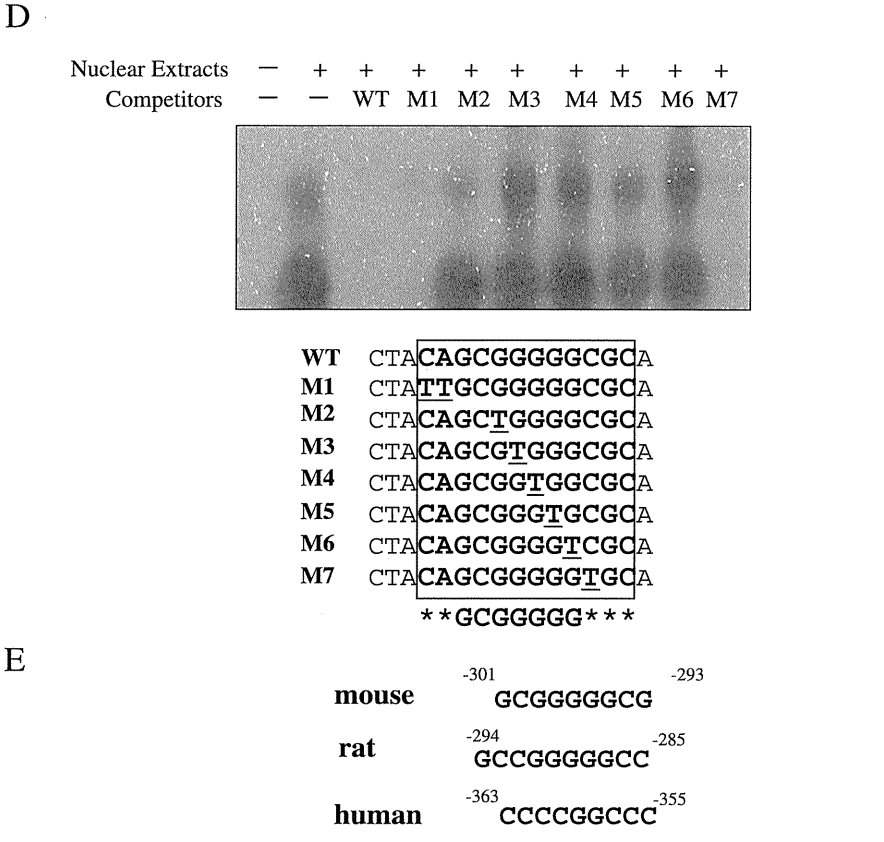

Fig. 2 (*continued*).

inserts were cut out with *Sma*I/*Kpn*I and inserted into the *Sma*I/*Kpn*I digested pRBGP3 (Tahara et al., 2004a,b).

For expression of mouse Egr-1 in mammalian cells, Egr-1 cDNA was obtained by PCR from the mouse liver cDNA library using primers 5'-AATCTAGAGCAGCGGCCAAGGCCGA-3' and 5'-AAAAGCTTCCCTTTAG-CAAATTTCA-3'. The resulting amplicon was digested with *Xba*I and *Hind*III and inserted into *Xba*I/*Hind*III digested pCG-N-HA (Mizutani et al., 2002). The mouse NAB1 cDNA was amplified by PCR from mouse

kidney cDNA library using primers 5'-AAAAGCTTGCCACAGCCTTACC-TAGGA-3' and 5'- AATCTAGACTATCTTGAGTCTTCAGGC -3'. The resulting amplicon was digested with *Hind*III/*Xba*I and subcloned into *Hind*II/*Xba*I digested p3×FLAG-CMV-10 (SIGMA-ALDRICH, Tokyo, Japan). The sequence and insert orientation were confirmed by DNA sequence analysis.

2.4. Reporter gene assays

NIH3T3 cells were transfected with the reporter plasmids and pRL-CMV (Promega Co.), using a Hilymax reagent (Dojin. Co. Ltd. Tokyo, Japan) for 4 h, according to the manufacturer's recommendations. We also cotransfected these plasmids plus pCG-N-HA-Egr-1 or p3×FLAG-CMV-

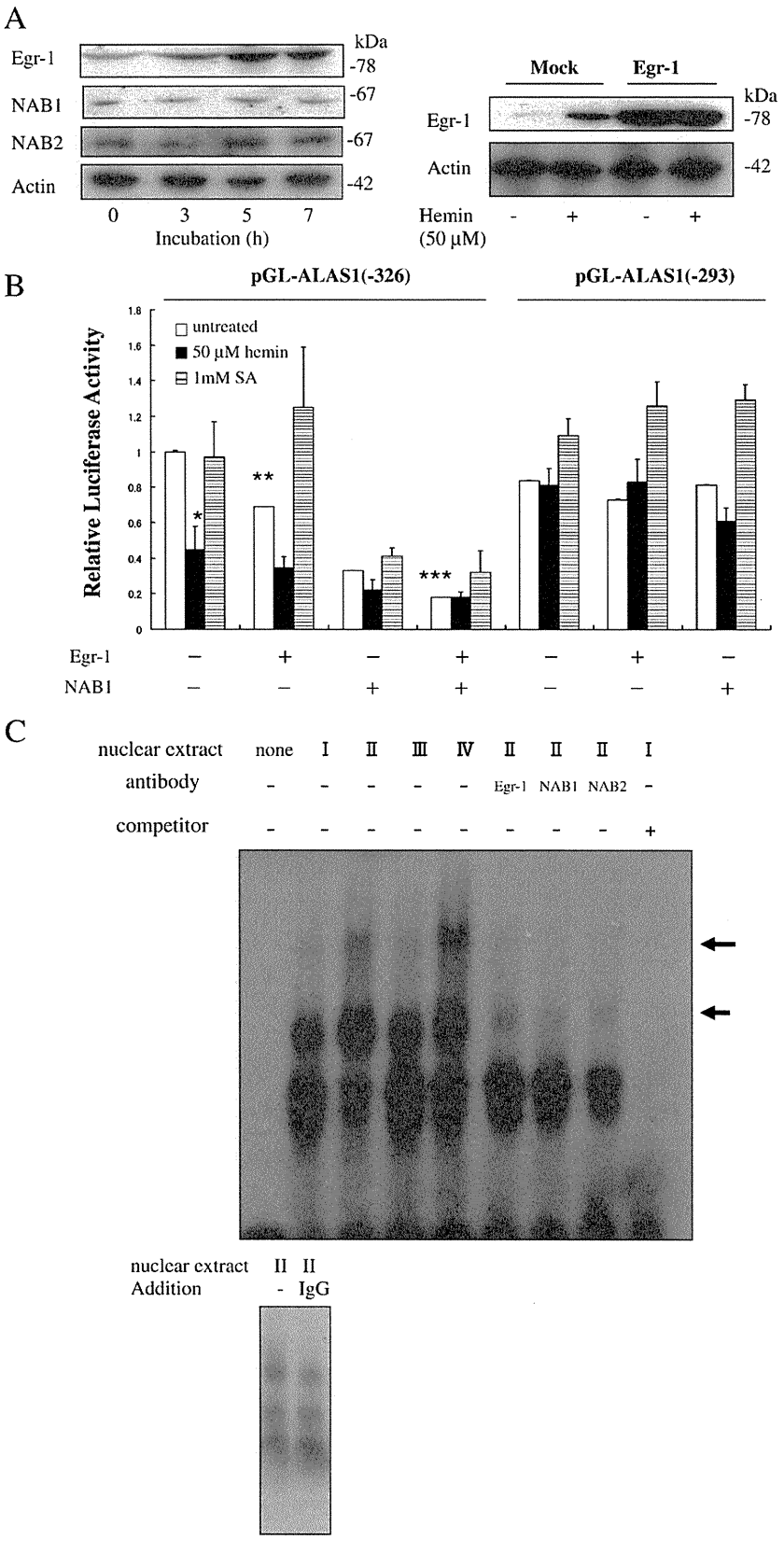

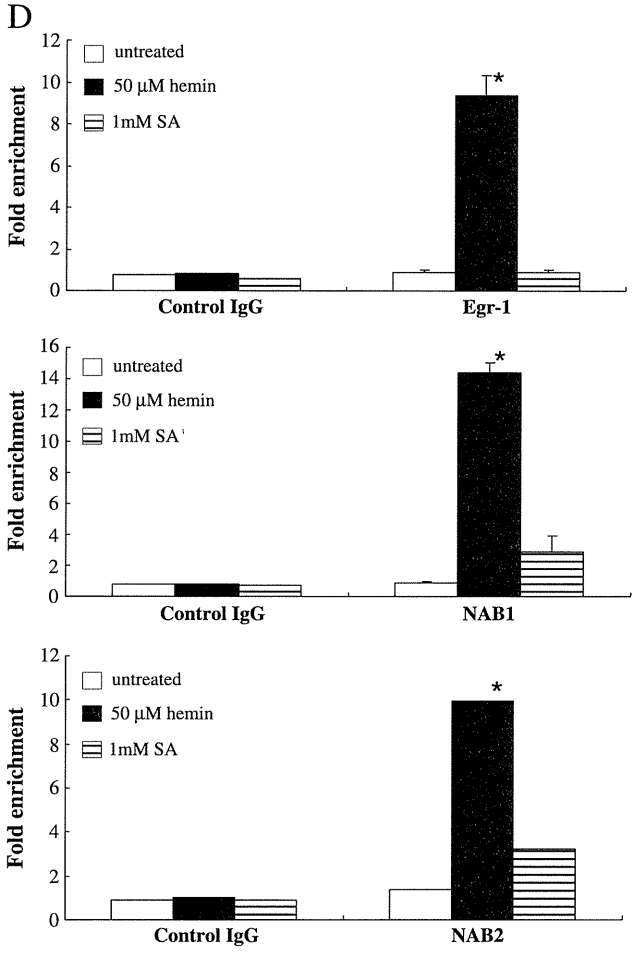

Fig. 3. Repression of the transcriptional activity of ALAS1-HRE by Egr-1, NAB1 and NAB2. (A) Left panel. Immunoblot analysis of the expression of the mouse Egr-1, NAB1 and NAB2 in hemin-treated NIH3T3 cells. The cells were treated in DMEM with 10 μM hemin for the indicated period. Right panel. The cells transfected with mock DNA and pCG-HA-Egr-1 were incubated for 16 h and then treated without or with 10 μM hemin for 5 h. The cellular proteins were separated by SDS-PAGE, followed by immunoblotting. The experiments were performed several times and the representative data are shown. (B) The transcriptional activity of Egr-1 and NAB1 for the ALAS1-HRE. NIH3T3 cells were transfected with pGL-ALAS1(−326) or pGL-ALAS1(−293) and plasmids carrying Egr-1 or NAB1. The cells were treated without or with 50 μM hemin and/or 1 mM SA for 16 h. Luciferase activity was measured and normalized to *Renilla* luciferase activity. The data are the average ± SEM for at least three independent experiments (*$P<0.01$, hemin treatment versus vehicle control; **$P<0.01$, Egr-1 overexpressing cells versus control cells; ***$P<0.005$, Egr-1 and NAB1 overexpressing cells versus control cells). (C) EMSA of the ALAS1-HRE oligonucleotides-binding activity in hemin- or SA-treated Hepa1-6 cells. EMSA was performed with nuclear extracts from the cells treated with 50 μM hemin and/or 1 mM SA using ^{32}P-labeled ALAS1-HRE. A 50-fold excess amount of unlabeled ALAS1-HRE oligonucleotide was used as a competitor. EMSA was carried out using the reaction mixture incubated with ^{32}P-labeled ALAS1-HRE at 4 °C for 10 min. The preincubation of nuclear extracts with antibodies for Egr-1, NAB1 or NAB2 was carried out at 4 °C for 20 min. Complexes were separated using 4% polyacrylamide gel. Nuclear extracts from untreated (I), and hemin (II)-, SA (III)- and hemin plus SA (IV)-treated cells were used. Arrows show the positions of the bands increasing by the hemin treatment (upper panel). Lower panel shows EMSA with nuclear extracts (II) preincubated with normal rabbit IgG (IgG). (D) Effect of hemin or SA on the occupancy of the ALAS1 promoter by Egr-1 (upper panel), NAB1 (middle panel) and NAB2 (lower panel). ChIP assay was performed with lysates from Hepa1-6 cells treated with 50 μM hemin and/or 1 mM SA for 16 h. Real-time PCR was performed to amplify the mouse ALAS1 promoter region containing ALAS1-HRE. Data are represented as fold enrichment compared to IgG control (*$P<0.001$, hemin treatment versus vehicle control).

10-NAB1. The cells were incubated with 50 μM hemin or 1 mM SA for 16 h. Dual-luciferase reporter assay system was used for measuring luciferase activity, and relative light units (RLU) represent *Firefly* luciferase normalized against *Renilla* luciferase activity (Tahara et al., 2004a,b).

2.5. Electrophoretic mobility shift assays (EMSA)

Nuclear extracts were prepared from cultured cells by the method of Schreiber et al. (1989). The radiolabeled probe CTACAGCGGGGGCGCA was phosphorylated at the 5'-end with [γ-^{32}P]ATP and T4 polynucleotide kinase and annealed with equimolar amount of CTACAGCGGGGGCGCA. EMSA was carried out as described previously (Gotoh et al., 2008). The reaction mixtures were separated on a 4% polyacrylamide. After electrophoresis, the gels were exposed to X-ray film at -80 °C. The oligonucleotides containing mutated sites used in competition experiments were as follows: 5'-CTATTGCGGGGGCGCA-3' and 5'-TGCGCCCCCGCAATAG-3'. (M1); 5'-CTACAGCTGGGGCGCA-3' and 5'-TGCGCCCCAGCTGTAG-3' (M2); 5'-CTACAGCGTGGGCGCA-3' and 5'-TGCGCCCACGCTGTAG-3' (M3); 5'-CTACAGCGGTGGCGCA-3' and 5'-TGCGCCACCGCTGTAG-3' (M4); 5'-CTACAGCGGGTGCGCA-3' and 5'-TGCGCACCCGCTGTAG-3' (M5); 5'-CTACAGCGGGGTCGCA-3' and 5'-TGCGACCCCGCTGTAG-3' (M6); and 5'-CTACAGCGGGGGTGCA-3' and 5'-TGCACCCCCGCTGTAG-3' (M7).

2.6. Reverse transcriptase (RT)-PCR analysis

Total RNA was isolated from the cells by the guanidium isothiocyanate method (Taketani et al., 2003). Single strand cDNA derived from the RNA was synthesized with the oligo(dT) primer, using ReveTra Ace (Toyobo, Co.), followed by PCR, using the indicated primers. The cDNAs obtained were analyzed using a 1.1% agarose gel. The DNA amount in the gel was quantified using Image J software. The primers were 5'-GGAACCATGCCTCCATGA-3' (forward) and 5'-GTTCTTAGCAGCATCGGC-3' (reverse) for ALAS1 and 5'-TGGGTGTGAACCACGAGA-3' (forward) and 5'-TTACTCCTTGGAGGCCATG-3' (reverse) for GAPDH. The amount of cDNA added to the reaction mixture was normalized by the intensity of GAPDH amplicon.

2.7. Immunoblotting

The lysates from NIH3T3 cells were subjected to SDS-PAGE and electroblotted onto PVDF membrane (Bio-Rad Laboratories, Hercules, CA). Immunoblotting was carried out with antibodies for Egr-1, NAB1, NAB2 and actin as the primary antibodies (Tahara et al., 2004a; Gotoh et al., 2008).

2.8. ChIP assay

Hepa1-6 cells (1×10^8) were cross-linked with 1% formaldehyde at room temperature for 15 min. Immunoprecipitation with anti-Egr-1, NAB1 and NAB2 antibodies, and control IgG was performed, followed by isolation of immunoprecipitates with protein A-Sepharose beads, as described (Tahara et al., 2004b; Gotoh et al., 2008). Primers 5'-CATGCAGCAAAGAAGGTCT-3' and 5'- ATATAGAGCCGGAGTGACC-3' were used to amplify the DNA fragment of the ALAS1 promoter (−455/−37) containing sequences of ALAS1 HRE (5'-GCGGGGGCG-3'). Real-time PCR was performed with a SYBR Green I kit (Toyobo Co.) and the Applied Biosystems 7500 real time PCR system.

2.9. Estimation of the intracellular level of heme

The level of heme in NIH3T3 cells (1×10^5) was estimated after conversion of heme to protoporphyrin, using a Hitachi MPF-4 fluorescence spectrophotometer (Taketani et al., 2003).

2.10. Statistics

Two-sample *t*-tests were used to compare the reporter activity, the amount of the protein–DNA complex and the level of ALAS1 mRNA between treated and untreated controls. Comparison of data from different treatment groups was conducted using one-way analysis of

variance (ANOVA). Analysis was performed using Microsoft Excel 2003 software.

3. Results

3.1. Identification of HRE in the mouse ALAS1 promoter

The expression of ALAS1 is known to be regulated by heme at a transcriptional level (Furuyama et al., 2007; Okano et al., 2010) and the level of ALAS1 mRNA in hemin-treated cells was markedly decreased (see Fig. 4A). To examine the heme-dependent transcriptional repression of the mouse *ALAS1* gene (Fig. 1A), we first carried out the reporter assay to find the heme-response in the distal region of the promoter of the mouse *ALAS1* gene. In the distal ALAS1 enhancer region (−3539/−2843 bp), two DR1-like sequences, the presumable binding sites of RXR (Gotoh et al., 2008) were found. We constructed the reporters containing these DR1-like sites, and transfected them into NIH3T3 cells. When we examined the luciferase reporter activity by the addition of hemin, virtually no change was observed (data not shown). We also found seven RORE-like sequences, the putative Rev-erbα binding site (Raghuram et al., 2007), from −8 to −4 kb upstream of the transcription start site and constructed two reporter plasmids containing −7760/−5970 and −5,976/−4,398 bp, but these reporters did not respond to heme even by coexpression of Rev-erbα (data not shown). Then we carefully examined the reporter activity within the proximal region of the mouse *ALAS1* gene promoter (−1241/+39). The luciferase activity of pGL-ALAS1p was decreased in hemin-treated cells, but slightly increased in the cells treated with SA, an inhibitor of heme biosynthesis, showing a heme-dependent repression (Fig. 1B). To find the heme-responsive region, sequential deletion of the promoter was carried out. We found that pGL-ALAS1(−302) exhibited a decrease by hemin and an increase by SA (Fig. 2A). The down regulation of the activity of pGL-ALAS1(−297) was weak or not observed with that of pGL-ALAS1 (−293), pGL-ALAS1(-177) and pGL-ALAS1(−62). To further examine the involvement of the region in heme-induced repression, we constructed the mutated reporter within the region −302/−293 and examined the effect of hemin on the transcriptional activity. Compared with the effect of hemin on the activities of pGL-ALAS1(−302), pGL-ALAS1(−302)mtA and pGL-ALAS1(−302)mtB showed the weak repression by hemin (Fig. 2B). These results indicated that the sequence (GCGGGGGCG) at −301/−293 corresponds to the HRE of the mouse *ALAS1* gene. To confirm the ALAS1-HRE (GCGGGGGCG), we connected tandem repeats of the double-stranded oligonucleotide to pRBGP3 carrying the minimal promoter. The resulting pALAS1 HRE (*x*2) and pALAS1 HRE (x4) showed the increase and decrease of the reporter activity in hemin- and SA-treated cells, respectively (Fig. 2C). Competitive assay of EMSA using ^{32}P-labeled HRE probe was carried out by the addition of an excess amount of mutated HRE fragments. As shown in Fig. 2D, the mutation of a single nucleotide inside of GCGGGGGC diminished the competition, indicated that the sequence of GGGGG in ALAS1-HRE was critically important in the heme repression. The GC-rich site corresponding to the putative ALAS1-HRE was found in the proximal promoter region of rat and human *ALAS1* gene (Fig. 2E).

3.2. Egr-1 and NAB1/2 complex binds to the ALAS1-HRE

Several transcription factors including Sp family and Egr-1 were found to bind to the GC-rich sequence of the gene promoter. Especially, Egr-1 functions in transcription of external stimuli and responds to oxidative stress such as ischemia/reperfusion, hypoxia, and heme. Then we examined the role of Egr-1 toward the heme repression through ALAS1-HRE. Immunoblot analysis showed that the expression of Egr-1 was rapidly increased by the treatment with hemin while those of NAB1 and NAB2, corepressors of Egr-1, did not change in hemin-treated cells (Fig. 3A). The analysis by RT-PCR

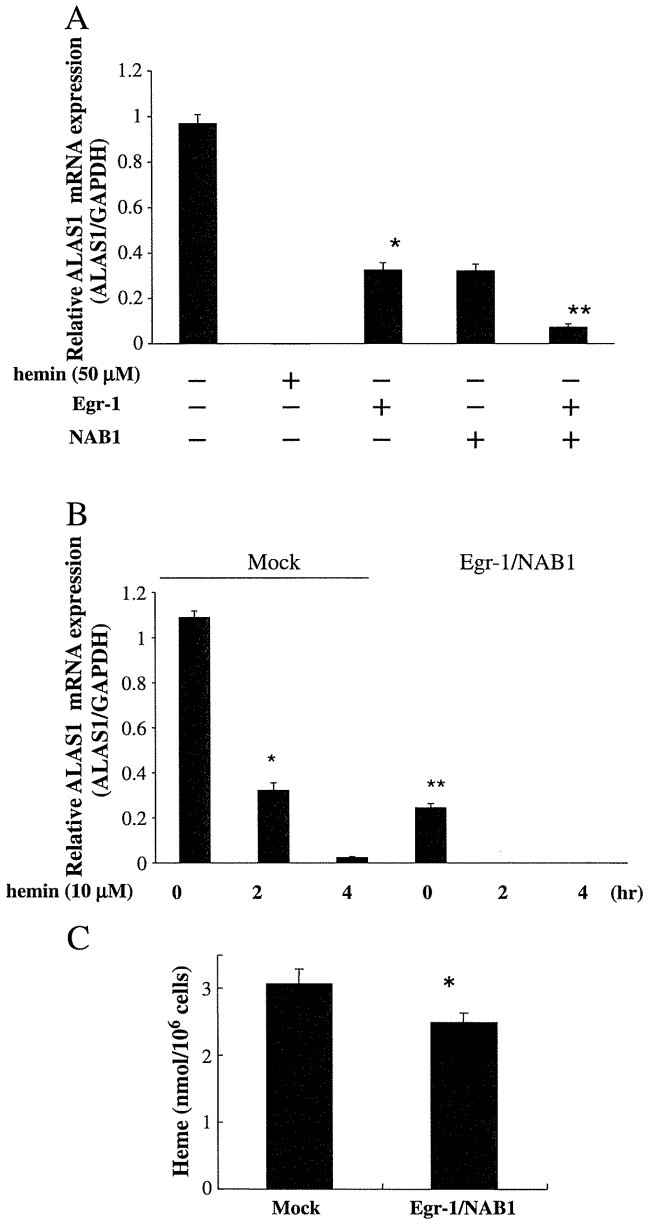

Fig. 4. Effect of the expression of Egr-1 and NAB1 on the levels of ALAS1 mRNA and intracellular heme. (A) RT-PCR analysis of the mouse ALAS1 mRNA in NIH3T3 cells overexpressing Egr-1 and NAB1. Cells were cotransfected with pCG-HA-Egr-1 and p3x-Flag-NAB1, followed by the treatment with 50 μM hemin for 16 h. RNA was isolated, and RT-PCR was carried out. The products were separated using an agarose gel. The DNA amount in the gel was quantified with Image J software (*P<0.01, Egr-1 overexpressing cells versus control cells; **P<0.001, Egr-1 and NAB1 overexpressing cells versus control cells). (B) Time course of the level of the ALAS1 mRNA in hemin-treated cells. The cells cotransfected with the indicated plasmid were cultured for 16 h and treated with 10 μM hemin in FCS-free medium. *P<0.01, hemin treatment versus control; **P<0.01, Egr-1 and NAB1 overexpressing cells versus control cells. (C) The intracellular level of heme in NIH3T3 cells overexpressing Egr-1 and NAB1. The cells were transfected with plasmids carrying Egr-1 and NAB1. After 24 h cultivation, the cells were washed twice with PBS and collected. The content of heme in cells was estimated after the conversion of heme to protoprphyrin. The data are the average ± SEM for five independent experiments (*P<0.01, treated versus vehicle control).

revealed that Egr-1 mRNA was increased by hemin treatment (data not shown), indicating that the induction of Egr-1 by heme is regulated at the transcriptional level. These results indicated that the expression of Egr-1 was controlled in response to the intracellular level of heme. The amount of Egr-1 in NIH3T3 cells was increased by the transfection with pCG-HA-Egr-1 (Fig. 3A). To investigate the involvement of Egr-1–NABs complexes in the heme-dependent

repression of the ALAS1 gene, reporter assay carrying ALAS1-HRE was carried out (Fig. 3B). When Egr-1 and NAB1 were overexpressed, the reporter activity of pGL-ALAS1(−326) decreased while that of pGL-ALAS1(−293) did not (Fig. 3B). The treatment of the cells over-expressing Egr-1 with hemin resulted in marked decrease of the reporter activity of pGL-ALAS1(−326), indicating that the activity is decreased dependent on the increase in the expression of Egr-1. We then conducted an EMSA of a synthetic oligonucleotide probe containing mouse ALAS1-HRE, using nuclear extracts of hemin- and SA-treated cells. Increases in the bindings corresponding to two bands to the nuclear extracts of hemin-treated cells were observed while the level of the binding slightly increased with the nuclear extracts of SA-treated cells (Fig. 3C). The upper bands disappeared upon preincubation of the nuclear extracts with anti-Egr-1, anti-NAB1 and anti-NAB2, but not with control IgG. These results indicated that the binding complex was composed of Egr-1 and NAB1/2. The status of the endogenous transcription complexes present on the ALAS1-HRE was determined by ChIP assay. The presence of the ALAS1-HRE in the chromatin immunoprecipitates was analyzed by semiquantitative PCR using specific pairs of primers spanning the ALAS1-HRE of the mouse *ALAS1* gene. As shown in Fig. 3D, Egr-1 was bound to ALAS1-HRE, and an increase in the binding of Egr-1 was observed when cells were treated with 50 μM hemin. The binding of NAB1/2 to ALAS1-HRE increased in parallel in the same cells. The increases of these factors were cancelled by treatment with 1 mM SA. These results, thereby, indicated that Egr-1 and NAB1/2 were involved in the repression of the expression of the mouse ALAS1 by heme.

3.3. Heme-dependent repression of the expression of *ALAS1* gene via Egr-1 and NAB1

To verify the involvement of Egr-1 and NABs in the repression of the expression of the mouse ALAS1, we examined the expression of ALAS1 in pCG-HA-Egr-1 and p3x-Flag-NAB1-transfected cells. As shown in Fig. 4A, the level of ALAS1 mRNA was down-regulated by coexpressions of Egr-1 and NAB1. When the cells coexpressing Egr-1 and NAB1 were treated with 10 μM hemin, the expression of ALAS1 mRNA was rapidly decreased (Fig. 4B). Finally, the expression of Egr-1 and NAB1 led to a decrease of the intracellular level of heme (Fig. 4C). Taken together, the Egr-1–NABs complex occupied the ALAS1-HRE of the promoter of the mouse *ALAS1* gene in response to heme and reduced the expression of ALAS1.

4. Discussion

The present study showed that Egr-1 plays an important role in the regulation of heme biosynthesis and directly represses the expression of ALAS1 by heme. The expression of ALAS1 mRNA was markedly reduced when the content of heme in mouse NIH3T3 cells was increased by treatment with hemin. In contrast, exogenously added SA slightly increased the level of ALAS1 mRNA. These findings were similar to previous observations that the expression of ALAS1 in non-erythroid cells was reduced when these cells were cultured with hemin (Okano et al., 2010) and support the negative feedback effect of heme on heme biosynthesis (Furuyama et al., 2007). Using a promoter assay of the mouse *ALAS1* gene, the present study confirmed that the expression of ALAS1 mRNA is regulated by hemin at the transcriptional level. There are also many reports that heme reduces the expression of ALAS1 protein by the coordinate regulation of posttranslational events such as the stability of ALAS1 mRNA, the import of precursor ALAS1 into mitochondria and the enzyme activity (Lathrop and Timko, 1993; Munakata et al., 2004). We have shown for the first time that the heme-dependent repression of the expression of mouse ALAS1 at the transcriptional level occurred in the proximal promoter region of *ALAS1* gene where is interacted with Egr-1. The decrease of ALAS1 mRNA was dependent on the level of Egr-1, but the decrease by hemin treatment was greater than that in Egr-1 and NAB1 overexpressing cells (Figs. 3A and 4A), suggesting that heme not only negatively regulates the transcription of the ALAS1 gene but also reduces the stability of ALAS1 mRNA.

Other investigators (Fraser et al., 2003; Handschin et al., 2005; Peyer et al., 2007) have shown that several transcription factors including nuclear receptors CAR, PXR, FXR and HNF4α as well as the coactivator PGC-1α mediate the transcriptional regulation of ALAS1 to various stumuli such as fasting, or upon the exposure to endo- and xenobiotics. Since it is recently reported that ALAS1 expression is repressed by heme at a transcriptional level, mediating by recently identified nuclear receptors such as Rev-erbα (Yin et al., 2007; Wu et al., 2009), we tried to identify the site of the enhancer region involved of nuclear receptors in down-regulation of the expression of the mouse ALAS1 transcription, which is exerted by the end product heme. The reporters carrying the repeats of DR1 or RORE-like region (−8 to −2.8 kb) were constructed, and the effect of heme on the luciferase activity was examined. As far as we examined, we failed in the detection of the involvement of heme in the decrease of the transcriptional activity in these regions even by the expression of Rev-erbα. On the other hand, a heme-dependent decrease of the ALAS1 promoter activity was found in the proximal region (−301 to −293b), a finding consistent with the previous observations with the rat ALAS1 promoter (Varone et al., 1999).

The expression of ALAS1 is known to circadian, regulated by NPAS2, a heme-binding circadian factor and PGC-1α (Yin et al., 2007). In addition to repressive function of Rev-erbα (Wu et al., 2009), this feedback loop may control heme biosynthesis. However, this model seems to be an indirect regulation which is necessary for de novo protein synthesis. Additionally, the present study showed the direct effect of heme on the transcription of *ALAS1* gene, by regulating the binding of Egr-1 and NAB1/2 on the mouse ALAS1 promoter located at −301/−293. The EMSA with mutated competitors of mutants and reporter assays revealed that the sequence GCGGGGGCG was designated as mouse ALAS1-HRE. Interestingly, the possible ALAS1-HRE is found in the proximal region of the promoter of mammalian *ALAS1* gene. Varone et al. (1999) reported the GC rich regions which correspond to the putative AP-2 binding sites in proximal site of rat ALAS1 promoter, and these may contribute to the heme-dependent repression of the gene. Using chromatin immunoprecipitations, we found that the recruitments of Egr-1 and NAB1/2 to the ALAS1-HRE increased in hemin-treated cells. When we examined the involvement of AP-2 in the transcriptional activity of ALAS1-HRE, an increase in the activity by expression of AP-2α was observed (data not shown). Considering that the molecular and functional interactions of AP-2 with Egr-1 were found in the GC rich region of some genes (Imhof et al., 1999; Dabir et al., 2008), AP-2 and Egr-1 may share the HRE, and effectively compete with them. Therefore, in addition of contribution of Rev-erbα to the repressive effect on the enhancer region of *ALAS1* gene, Egr-1/NABs are involved in the heme-dependent repression at the proximal region of ALAS1 promoter.

There are several transcription factors such as Sp and Egr families recognizing GC-rich sequences (Imhof et al., 1999; Blaschke et al., 2004). Members of Egr family play diverse physiological roles and have negative and positive effects on growth. The NAB1 and NAB2, major transcriptional corepressors of Egr-1, directly interact with a conserved domain found in Egr-1 and repress the activation of the various target promoters (Houston et al., 2001; Kumbrink et al., 2005). We now demonstrated that the binding of Egr-1 as well as NAB1/2 complex to the ALAS1-HRE was increased by the treatment of the cells with hemin. We also found that overexpressions of Egr-1 and NAB1 resulted in decreases of the expression of ALAS1 mRNA and the intracellular level of heme. It is known that Egr-1 was induced by various stimuli including inflammation, ROS/oxidative stress, hypoxia and hyperoxia (Blaschke et al., 2004; Khachigian, 2006). Consistent with a recent finding that heme up-regulates the expression of Egr-1

(Hasan and Schafer, 2008), the present data showed that the level of Egr-1 was rapidly increased in hemin-treated cells (Fig. 3A), indicating a underlying mechanism for regulating the repressive function of Egr-1 and NAB1/2 complex in response to intracellular heme level. Thus, induced Egr-1 by heme provides down-regulation of the transcription of mouse ALAS1 via ALAS1-HRE. Moreover, since the expression of Egr-1 was regulated by multiple factors, it is possible that the Egr-1 binding site in the promoter of *ALAS1* gene can response to various factors as well as heme.

In summary, we have now identified the molecular mechanism of the heme-dependent transcriptional repression of ALAS1 via the regulation of Egr-1 and NABs. The exact functional correlates of the regulation of Egr-1 on the expression of ALAS1 are likely to be more complex, and the mechanisms involved in the increase in the recruitment of Egr-1 to the ALAS1-HRE by heme are unclear. These will require further investigations using in vitro and in vivo systems.

Acknowledgements

We thank Drs. Osamu Nakajima and Takashi Osumi for kind gifts of pANH III and pCMV-Rev-erbα, respectively, and Ikuko Sagami for valuable suggestions. This study was partially supported by grants by KIT and JST.

References

Blaschke, F., Bruemmer, D., Law, R.E., 2004. Egr-1 is a major vascular pathogenic transcription factor in atherosclerosis and restenosis. Rev. Endocr. Metab. Disord. 5, 249–254.

Dabir, P., Marinic, T.E., Krukovets, I., Stenina, O.I., 2008. Aryl hydrocarbon receptor is activated by glucose and regulates the thrombospondin-1 gene promoter in endothelial cells. Circ. Res. 102, 1558–1565.

Fraser, D.J., Zumsteg, A., Meyer, U.A., 2003. Nuclear receptors constitutive androstane receptor and pregnane X receptor activate a drug-responsive enhancer of the murine 5-aminolevulinic acid synthase gene. J. Biol. Chem. 278, 39392–39401.

Furuyama, K., Kaneko, K., Vargas, P.D., 2007. Heme as a magnificent molecule with multiple missions: heme determines its own fate and governs cellular homeostasis. Tohoku J. Exp. Med. 213, 1–16.

Gashler, A.L., Swaminathan, S., Sukhatme, V.P., 1993. A novel repression module, an extensive activation domain, and a bipartite nuclear localization signal defined in the immediate-early transcription factor Egr-1. Mol. Cell. Biol. 13, 4556–4571.

Gotoh, S., Ohgari, Y., Nakamura, T., Osumi, T., Taketani, S., 2008. Heme-binding to the nuclear receptor retinoid X receptor alpha (RXRalpha) leads to the inhibition of the transcriptional activity. Gene 423, 207–214.

Handschin, C., et al., 2005. Nutritional regulation of hepatic heme biosynthesis and porphyria through PGC-1alpha. Cell 122, 505–515.

Hasan, R.N., Schafer, A.I., 2008. Hemin upregulates Egr-1 expression in vascular smooth muscle cells via reactive oxygen species ERK-1/2-Elk-1 and NF-kappaB. Circ. Res. 102, 42–50.

Houston, P., Campbell, C.J., Svaren, J., Milbrandt, J., Braddock, M., 2001. The transcriptional corepressor NAB2 blocks Egr-1-mediated growth factor activation and angiogenesis. Biochem. Biophys. Res. Commun. 283, 480–486.

Imhof, A., et al., 1999. Transcriptional regulation of the AP-2alpha promoter by BTEB-1 and AP-2rep, a novel wt-1/egr-related zinc finger repressor. Mol. Cell. Biol. 19, 194–204.

Kaasik, K., Lee, C.C., 2004. Reciprocal regulation of haem biosynthesis and the circadian clock in mammals. Nature 430, 467–471.

Khachigian, L.M., 2006. Early growth response-1 in cardiovascular pathobiology. Circ. Res. 98, 186–191.

Kramer, M.K., Gunaratne, P., Ferreira, G.C., 2000. Transcriptional regulation of the murine erythroid-specific 5-aminolevulinate synthase gene. Gene 247, 153–166.

Kumbrink, J., Gerlinger, M., Johnson, J.P., 2005. Egr-1 induces the expression of its corepressor nab2 by activation of the nab2 promoter thereby establishing a negative feedback loop. J. Biol. Chem. 280, 42785–42793.

Lathrop, J.T., Timko, M.P., 1993. Regulation by heme of mitochondrial protein transport through a conserved amino acid motif. Science 259, 522–525.

Mizutani, A., Furukawa, T., Adachi, Y., Ikehara, S., Taketani, S., 2002. A zinc-finger protein, PLAGL2, induces the expression of a proapoptotic protein Nip3, leading to cellular apoptosis. J. Biol. Chem. 277, 15851–15858.

Munakata, H., et al., 2004. Role of the heme regulatory motif in the heme-mediated inhibition of mitochondrial import of 5-aminolevulinate synthase. J. Biochem. 136, 233–238.

Okano, S., et al., 2010. Indispensable function for embryogenesis, expression and regulation of the nonspecific form of the 5-aminolevulinate synthase gene in mouse. Genes Cells 15, 77–89.

Peyer, A.K., et al., 2007. Regulation of human liver delta-aminolevulinic acid synthase by bile acids. Hepatology 46, 1960–1970.

Raghuram, S., et al., 2007. Identification of heme as the ligand for the orphan nuclear receptors REV-ERBalpha and REV-ERBbeta. Nat. Struct. Mol. Biol. 14, 1207–1213.

Rokosh, G., 2008. Heme Egr-1: new partners in atherosclerotic progression? Circ. Res. 102, 6–8.

Sassa, S., 1988. Heme stimulation of cellular growth and differentiation. Semin. Hematol. 25, 312–320.

Schreiber, E., Matthias, P., Müller, M.M., Schaffner, W., 1989. Rapid detection of octamer binding proteins with 'mini-extracts,' prepared from a small number of cells. Nucleic Acids Res. 17, 6419.

Schuurmans, M.M., Hoffmann, F., Lindberg, R.L., Meyer, U.A., 2001. Zinc mesoporphyrin represses induced hepatic 5-aminolevulinic acid synthase and reduces heme oxygenase activity in a mouse model of acute hepatic porphyria. Hepatology 33, 1217–1222.

Svaren, J., Sevetson, B.R., Apel, E.D., Zimonjic, D.B., Popescu, N.C., Milbrandt, J., 1996. NAB2, a corepressor of NGFI-A (Egr-1) and Krox20, is induced by proliferative and differentiative stimuli. Mol. Cell. Biol. 16, 3545–3553.

Tahara, T., Sun, J., Igarashi, K., Taketani, S., 2004a. Heme-dependent up-regulation of the alpha-globin gene expression by transcriptional repressor Bach1 in erythroid cells. Biochem. Biophys. Res. Commun. 32, 77–85.

Tahara, T., et al., 2004b. Heme positively regulates the expression of beta-globin at the locus control region via the transcriptional factor Bach1 in erythroid cells. J. Biol. Chem. 279, 5480–5487.

Taketani, S., Kakimoto, K., Ueta, H., Masaki, R., Furukawa, T., 2003. Involvement of ABC7 in the biosynthesis of heme in erythroid cells: interaction of ABC7 with ferrochelatase. Blood 101, 3274–3280.

Varone, C.L., Giono, L.E., Ochoa, A., Zakin, M.M., Cánepa, E.T., 1999. Transcriptional regulation of 5-aminolevulinate synthase by phenobarbital and cAMP-dependent protein kinase. Arch. Biochem. Biophys. 372, 261–270.

Wu, N., Yin, L., Hanniman, E.A., Joshi, S., Lazar, M.A., 2009. Negative feedback maintenance of heme homeostasis by its receptor, Rev-erbalpha. Genes Dev. 23, 2201–2209.

Yin, L., et al., 2007. Rev-erbalpha, a heme sensor that coordinates metabolic and circadian pathways. Science 318, 1786–1789.